Blocking palmitoylation of *Toxoplasma gondii* myosin light chain 1 disrupts glideosome composition but has little impact on parasite motility

Pramod K. Rompikuntal[1], Ian T. Foe[2], Bin Deng[4,5], Matthew Bogyo[2,3], Gary E. Ward[1*]

[1]Department of Microbiology and Molecular Genetics, University of Vermont Larner College of Medicine, Burlington, VT 05405, USA

[2]Department of Pathology, Stanford University School of Medicine, Stanford, CA 94305, USA

[3]Department of Microbiology and Immunology, Stanford University School of Medicine, Stanford, CA 94305, USA

[4]Department of Biology & [5]Vermont Genetics Network Proteomics Facility, University of Vermont, Burlington VT 05405, USA

* Corresponding author: Tel: (802) 656-4868, e-mail: gary.ward@uvm.edu

Abstract

Toxoplasma gondii is a widespread apicomplexan parasite that causes severe disease in immunocompromised individuals and the developing fetus. Like other apicomplexans, *T. gondii* uses an unusual form of gliding motility to invade cells of its hosts and to disseminate throughout the body during infection. It is well established that a myosin-based motor consisting of a Class XIVa heavy chain (TgMyoA) and two light chains (TgMLC1 and TgELC1/2) plays an important role in parasite motility. The ability of the motor to generate force at the parasite periphery is thought to be reliant upon its anchoring and immobilization within a peripheral membrane-bound compartment, the inner membrane complex (IMC). The motor does not insert into the IMC directly; rather, this interaction is believed to be mediated by the binding of TgMLC1 to the IMC-anchored protein, TgGAP45. The binding of TgMLC1 to TgGAP45 is therefore considered a key element in the force transduction machinery of the parasite. TgMLC1 is palmitoylated, and we show here that palmitoylation occurs on two N-terminal cysteine residues, C8 and C11. Mutations that block TgMLC1 palmitoylation disrupt the association of TgMLC1 with the membrane fraction of the parasite in phase partitioning experiments and completely block the binding of TgMLC1 to TgGAP45. Surprisingly, the loss of TgMLC1 binding to TgGAP45 in these mutant parasites has little effect on their ability to initiate or sustain movement. These results question a key tenet of the current model of apicomplexan motility and suggest that our understanding of gliding motility in this important group of human and animal pathogens is not yet complete.

Importance

Gliding motility plays a central role in the life cycle of *T. gondii* and other apicomplexan parasites. The myosin motor thought to power motility is essential for virulence but distinctly

different from the myosins found in humans. Consequently, an understanding of the mechanism(s) underlying parasite motility and the role played by this unusual myosin may reveal points of vulnerability that can be targeted for disease prevention and treatment. We show here that mutations that uncouple the motor from what is thought to be a key structural component of the motility machinery have little impact on parasite motility. This finding runs counter to predictions of the current, widely-held "linear motor" model of motility, highlighting the need for further studies to fully understand how apicomplexan parasites generate the forces necessary to move into, out of and between cells of the hosts they infect.

Introduction

Toxoplasmosis is among the most widespread and common parasitic infections of humans (1). Acute infection, while typically subclinical and self-limiting, can cause life-threatening disease in immunocompromised individuals and the developing fetus. The causative agent of toxoplasmosis is the protozoan parasite, *Toxoplasma gondii*. *T. gondii* and other parasites of the phylum Apicomplexa, including those that cause malaria and cryptosporidiosis, use an unusual form of substrate-dependent gliding motility to invade into and egress from host cells, migrate across biological barriers, and disseminate through the infected host's tissues (2-4).

Gliding motility in apicomplexan parasites is controlled, at least in part, by an unconventional class XIVa myosin, MyoA (5-15). According to the "linear motor" model of motility that has dominated the field for the last decade (reviewed in (16); see Fig. 1A), *T. gondii* MyoA (TgMyoA) and its associated light chains (TgMLC1 and either TgELC1 or TgELC2) are anchored to the parasite's inner membrane complex (IMC) via the acylated glideosome-

58 associated protein, TgGAP45. TgGAP45, in turn, binds to the transmembrane proteins TgGAP40
59 and TgGAP50. TgGAP50 is firmly immobilized within the IMC lipid bilayer, potentially serving
60 as a fixed anchor against which the motor complex can generate force (17, 18). This large,
61 heterooligomeric protein complex (TgMyoA, its light chains, TgGAP40, TgGAP45 and
62 TgGAP50) is referred to as "the glideosome". In the linear motor model, short actin filaments
63 located between the parasite plasma membrane and the IMC are connected to ligands on the
64 substrate through a glideosome-associated connector protein (GAC; (19)) that binds to the
65 cytosolic tails of surface adhesins. Because the motor is anchored into the IMC, when the motor
66 displaces the fixed actin filaments rearward, the parasite moves forward relative to the substrate
67 (Fig. 1A).

68 TgMLC1 is thought to play two key roles within the *T. gondii* glideosome. First, TgMLC1 binds
69 to the C-terminal tail of TgMyoA to reinforce the motor's lever arm (10, 13, 20). The lever arm
70 amplifies small motions at the myosin active site into larger movements that are capable of
71 displacing actin filaments (10, 21). Consistent with this proposed function, recombinant
72 TgMyoA is inactive in *in vitro* motility assays in the absence of TgMLC1 ((10) and unpublished
73 data). Second, an interaction between the N-terminal portion of TgMLC1 and the C-terminal
74 portion of TgGAP45 is believed to be the critical link that tethers the motor to the IMC (Fig. 1A;
75 (22, 23). Given these proposed functions, is not surprising that TgMLC1 is an essential protein,
76 and parasites depleted of TgMLC1 are significantly impaired in 3D motility, invasion, and host
77 cell egress (24, 25).

78 While the importance of TgMyoA, TgMLC1 and the other glideosome components in motility is
79 well established, recent data have called into question whether they are organized and function as
80 described by the linear motor model and/or whether alternative motility mechanisms exist (24-

29). For example, the ability of apicomplexan parasites to rock back and forth on a substrate along their anterior to posterior axis (30-36) is hard to reconcile with the linear motor model, as is the ability of parasites engineered to lack key components of the glideosome to continue moving ((24-26); see also (37)). Given the central importance of motility in the parasite's life cycle and virulence, it is important to fully understand how these proteins work together to generate the forces required to drive parasite movement.

S-palmitoylation is the reversible covalent attachment of a 16-carbon saturated fatty acid via a thioester linkage to cysteine residues of integral and peripheral membrane proteins (38, 39). This widespread post-translational modification of proteins mediates membrane association and can regulate subcellular localization, trafficking, structure, stability and diverse aspects of protein function (38, 40-42). Palmitoylation is thought to play an important role in the biology of *T. gondii* and other apicomplexan parasites (43-54). Recent chemical proteomic studies identified several hundred putatively palmitoylated proteins in *T. gondii* (282 unique proteins in one study (54) and 401 in another (44)). Surprisingly, these proteins included all components of the glideosome, including TgMLC1 (44, 54).

TgMLC1 contains five cysteine residues (Fig. 1B), two of which (C8 and C11) are predicted by CSS-Palm 4.0 to be potential sites of palmitoylation. These two cysteines are found within the apicomplexan-specific N-terminal extension of TgMLC1 (Fig. 1B), which is the region of the protein that binds to TgGAP45 ((23); Fig. 1A). Given the important role that TgMLC1 is thought to play in TgMyoA function and motility, we sought to experimentally confirm C8 and/or C11 as the sites of TgMLC1 palmitoylation and to explore the phenotypic consequences of mutations that block this modification.

Results

Identification of the sites of palmitoylation on TgMLC1

To determine whether C8 and/or C11 are sites of palmitoylation on TgMLC1, we replaced the endogenous *TgMLC1* gene with mutant alleles that produce either single (C8S, C11S) or double (C[8,11]S) cysteine to serine mutations, rendering these sites non-palmitoylatable. Each mutant protein was also FLAG-tagged at its N-terminus (Fig. S1; see Table S1 for a list of parasite strains used in this study and their designations). A fourth parasite line expressing FLAG-tagged wild-type TgMLC1 was similarly generated (WT). To determine the effect (if any) of the mutations on TgMLC1 palmitoylation, WT, C8S, C11S and C(8,11)S parasites were grown in the palmitic acid analog, 17-octadecynoic acid (17-ODYA). FLAG-tagged TgMLC1 was then immunoprecipitated and subjected to SDS-PAGE. Because 17-ODYA contains a terminal alkyne group, it can be fluorescently tagged with rhodamine-azide through a copper-catalyzed cycloaddition reaction; the amount of rhodamine bound to proteins in the immunoprecipitate can then be visualized by fluorescence scanning (54). The amount of rhodamine fluorescence associated with TgMLC1 (31 kDa) was significantly reduced in both the C8S and C11S mutants compared to WT, with C8S showing a greater reduction than C11S (Fig. 2). In the C(8,11)S double mutant, no 17-ODYA TgMLC1 labeling above background was detectable. In a previous study, C8 and/or C11 were speculated to be sites of palmitoylation on TgMLC1, and parasites expressing a second copy of TgMLC1 in which these two cysteines were mutated to alanines were generated (23). To compare our results to theirs, we generated a C(8,11)A allelic replacement line and found that, like the C(8,11)S double mutation, the C(8,11)A double

mutation completely blocked 17-ODYA labeling (Fig. 2). Taken together, these data identify C8 and C11 as essential for, and very likely the sites of, palmitoylation on TgMLC1.

Subcellular localization of non-palmitoylatable TgMLC1

TgMLC1 normally localizes uniformly around the parasite periphery (55). It was previously reported that the C(8,11)A double mutation caused TgMLC1 to mislocalize to the cytosol (23). It was therefore surprising that, in our hands, both the C(8,11)S and C(8,11)A mutant proteins remained localized at the parasite periphery (Fig. 3). Re-examination of the images shown in Frenal *et al.* (2010) revealed that most of the C(8,11)A mutant protein (named MLC1$^{CC\text{-}AA}$ in that study) was indeed also found at the parasite periphery, although there was a minor amount in the cytosol (for comparison, see the localization of a different mutant in that same study, MLC1-PGF^{AIA}, which was clearly cytosolic (23)). The fact that we detect little to no cytosolic staining with the C(8,11)A allele may reflect differences between the two studies in protein expression levels, since our mutant protein was expressed from the endogenous promoter at the endogenous locus whereas the previous study expressed the mutant gene in parasites also expressing the wild-type allele (23). Taken together, these data show that mutations that block TgMLC1 palmitoylation do not appreciably alter its localization at the parasite periphery.

Blocking palmitoylation of TgMLC1 alters its phase partitioning in Triton X-114

Next, we tested whether the mutations that block TgMLC1 palmitoylation within the parasite alter the phase partitioning of the protein in the non-ionic detergent Triton X-114 (TX-114). TX-114 efficiently solubilizes most proteins in the parasite at 4^{o}C; when subsequently warmed above the cloud point of the detergent (20^{o}C), intermicellar interactions cause the solution to separate into aqueous and detergent phases, which are enriched in hydrophilic and integral membrane

proteins, respectively (56, 57). WT, C8S and C11S TgMLC1 each partition roughly equally into the aqueous and detergent phases, but the C(8,11)S TgMLC1 double mutant is found almost entirely in the aqueous phase (Figs. 4A and S2), suggesting a lack of direct membrane association in the absence of palmitoylation. Similar results were seen with the C(8,11)A double mutant (Fig. 4A). As a control, the same samples were probed for TgGRA8, a dense granule protein (58) unrelated to TgMLC1. As expected, the phase partitioning of TgGRA8 was relatively unaffected by the TgMLC1 mutations (Figs. 4B and S2). These data suggest that the peripheral localization we observed for the C(8,11)S and C(8,11)A TgMLC1 mutants is likely mediated by interaction with other membrane-associated protein(s), rather than by a direct association with the lipid bilayer itself.

Effects of TgMLC1 palmitoylation on the composition of the glideosome

In the 17-ODYA labeling experiments, two prominently labeled ~50 kDa proteins were recovered in the FLAG-WT pulldowns in addition to FLAG-tagged TgMLC1, and these bands were not present in pulldowns from either the C(8,11)S or C(8,11)A double mutant (Fig. 2, asterisk). It was previously suggested that proteins of this size copurifying with WT TgMLC1 but not C(8,11)A might be other members of the glideosome complex (23). This hypothesis was strengthened by our subsequent observation that most, if not all, glideosome components are palmitoylated (54). We therefore analyzed the FLAG pulldowns of C8S, C11S and C(8,11)S parasites by western blot with antibodies against TgGAP45, TgELC1 and TgMyoA. As expected, TgGAP45 was recovered in the FLAG pulldown from parasites expressing WT TgMLC1; in striking contrast, virtually no TgGAP45 was recovered in FLAG pulldowns from parasites expressing C(8,11)S TgMLC1 (Fig. 5A). Pulldowns from parasites expressing the C8S and C11S single mutations contain intermediate levels of TgGAP45. Quantification of the

169 western blot signals confirmed these observations, and revealed that concomitant with the
170 decrease in TgGAP45 in the IP of the double mutant, there was a 2-3-fold increase in the amount
171 of TgELC1 and TgMyoA recovered (Fig. 5B). Similar results were seen with the C(8,11)A
172 mutant (Fig. S3). The lack of TgGAP45 in the IP from the double mutant is not due to changes in
173 TgGAP45 expression in this parasite line, as western blots of parasite lysate before
174 immunoprecipitation show similar amounts of TgGAP45 (Fig. 5A and S3, "input"). Similarly,
175 anti-TgMyoA western blots of whole parasite lysates reveals no changes in the level of
176 expression of TgMyoA in either the C(8,11)S or C(8,11)A mutant parasite lines (Fig. S4).
177 Blocking TgMLC1 palmitoylation seems to therefore block its ability to interact with TgGAP45,
178 while simultaneously increasing its interaction with TgMyoA and TgELC1.

179 **Effect of TgMLC1 palmitoylation on parasite motility**

180 Given the dramatic effect of the C(8,11)S double mutation on the binding of TgMLC1 to
181 TgGAP45, we expected to see a major impact on parasite motility. However, the motility of the
182 double mutant parasites was indistinguishable from parasites expressing WT TgMLC1 in terms
183 of motility initiation, mean displacement, mean speed and maximum speed (Fig. 6). Track
184 length was slightly shorter in the C(8,11)S parasites, but still reached 88% of WT levels. Thus,
185 parasites in which TgMLC1 has lost its ability to interact with TgGAP45 nevertheless show near
186 normal motility.

187 This result was unexpected since, according to the linear motor model of motility, disruption of
188 the interaction between TgMLC1 and TgGAP45 should uncouple TgMyoA from the IMC,
189 rendering it incapable of generating the force required for movement ((23); Fig. 1A). We
190 therefore investigated whether the near normal motility observed in the mutants could be due to

191 changes in the composition of the glideosome that could functionally compensate for the lack of
192 TgMLC1-TgGAP45 interaction, such as the association of TgGAP45 with an alternative light
193 chain/myosin motor, or interaction of either TgMLC1 or TgMyoA with alternative GAP
194 proteins.

195 First, we asked whether TgGAP45 associates with any new proteins in the absence of its normal
196 interaction with TgMLC1. Parasites expressing either WT or C(8,11)S TgMLC1 were
197 metabolically labeled with ^{35}S-methionine/cysteine and the labeled proteins that co-
198 immunoprecipitated with TgGAP45 were resolved by SDS-PAGE, transferred to a PVDF
199 membrane and visualized by phosphorimaging. The same membrane used for phosphorimaging
200 was subsequently processed for western blotting with antibodies against TgMyoA, TgGAP45
201 and TgMLC1 to determine which of the ^{35}S-labeled bands comigrate with which of the
202 glideosome proteins. As expected, both TgMyoA and TgMLC1 co-immunoprecipitate with
203 TgGAP45 from ^{35}S-labeled WT parasites, whereas neither protein is recovered in TgGAP5
204 pulldowns from C(8,11)S parasites (Fig. 7A), confirming that the motor does not bind to
205 TgGAP45 in the absence of TgMLC1 palmitoylation. No ^{35}S-labeled bands were detected in the
206 TgGAP45 pulldowns from C(8,11)S parasites that were not also present in the pulldowns from
207 WT parasites (Fig. 7A). TgGAP45 therefore does not appear to interact to any
208 significant/stoichiometric extent with alternate ^{35}S-labeled myosins or myosin light chains when
209 its interaction with TgMLC1 is disrupted by the C(8,11)S mutation.

210 We did a similar experiment to see if TgMyoA interacts with alternative GAP(s) (23) or other
211 proteins in the C(8,11)S mutant, proteins that might serve to anchor TgMyoA into the IMC in the
212 absence of a normal TgMLC1-TgGAP45 interaction. First, we Ty-tagged TgMyoA at the
213 endogenous *TgMyoA* locus in both the WT and C(8,11)S backgrounds using CRISPR/Cas9 (Fig.

S5). We then analyzed Ty pulldowns from ^{35}S-labeled WT and C(8,11)S parasites. Ty-tagged TgMyoA and associated TgMLC1 were recovered in the Ty pulldowns from both parasite lines and, as expected, TgGAP45 was only recovered in pulldowns from WT parasites (Fig. 7B). Again, no ^{35}S-labeled proteins were seen to associate with TgMyoA in the C(8,11)S parasites that were not also detected in WT parasites, so there is no evidence that TgMyoA interacts with new binding partners in the C(8,11)S double mutant (Fig. 7B).

Finally, we tested whether the mutant C(8,11)S TgMLC1 itself might interact with a different IMC-anchored protein(s) that could functionally compensate for its lack of interaction with TgGAP45. Anti-FLAG IPs from ^{35}S-labeled WT and C(8,11)S parasites again confirmed the western blotting results presented in Figs. 5 and S3: compared to WT TgMLC1, C(8,11)S TgMLC1 shows both a greatly reduced interaction with TgGAP45 and an increased interaction with TgMyoA (Fig. 7C; quantitative western blot results from the same sample are shown in Fig. S6). However, in this experiment we also saw a marked increase in the amount of an ~80kDa kDa ^{35}S-labeled protein co-immunoprecipitating with C(8,11)S TgMLC1 compared to WT TgMLC1 (Fig 7C, asterisk). This was intriguing since TgGAP80, a TgGAP45-related protein that normally interacts with TgMyoC, is also reportedly capable of interacting with TgMLC1 (59). This raised the possibility that an increased interaction between C(8,11)S TgMLC1 and TgGAP80 might functionally compensate for the loss of interaction between TgMLC1 and TgGAP45 in the mutant parasites. We therefore repeated the FLAG-TgMLC1 pulldowns on a preparative scale and determined the identity of each of the major bands recovered by LC/MS/MS (Fig. S7 and Tables S1-S10). The ~80kDa band proved to be a truncated form of TgMyoA rather than TgGAP80, and the increased levels of this TgMyoA fragment in the C(8,11)S pulldown paralleled the increased levels of full-length TgMyoA. Taken together, these

data argue that the near normal motility seen in C(8,11)S parasites cannot be explained by the binding of either TgGAP45 or components of the motor to alternative proteins that could functionally compensate for the lack of interaction between TgMLC1 and TgGAP45.

Discussion

The apicomplexan glideosome plays a critical role in parasite motility, invasion and virulence. Recent palmitome analyses have revealed that all known components of the *T. gondii* glideosome are palmitoylated, including TgMyoA, TgMLC1, TgELC1, TgGAP40, TgGAP45 and TgGAP50 (44, 54). Widespread glideosome palmitoylation has also been reported in *P. falciparum* (51, 60). Two of the *T. gondii* palmitoyl S-acyl transferases that are essential for parasite survival (TgDHHC2, TgDHHC14) localize to the IMC (61, 62) and are therefore well-situated to play a role in glideosome palmitoylation. The function of palmitoylation of one glideosome component, TgGAP45, was established in an elegant set of experiments by Frenal, Soldati-Favre and colleagues (23). Their study showed that C-terminal palmitoylation of TgGAP45 anchors its C-terminus in the IMC, while the other end of the protein is anchored in the plasma membrane via N-terminal palmitoylation and myristoylation. Acylation on the two ends of the protein therefore enables TgGAP45 to bridge the gap between the IMC and the plasma membrane; this determines the spacing between the two membranes and maintains the integrity of the parasite pellicle (23). The function of palmitoylation of other glideosome components is not known, and in most cases the specific residues palmitoylated on these other proteins have not been determined. We have focused here on the function of TgMLC1 palmitoylation.

In the linear motor model of motility, TgMLC1 plays two key roles in force generation: it stabilizes the TgMyoA lever arm (10, 13, 20), and it serves as a physical linker connecting the TgMyoA motor to TgGAP45 and the IMC (22, 23). We show here that TgMLC1 is dually palmitoylated, on C8 and C11 (Fig. 2). When we block palmitoylation by mutating these sites to either serine or alanine, TgMLC1 shows reduced association with the membrane fraction in phase-partitioning experiments (Fig. 4) and the mutant TgMLC1 no longer co-immunoprecipitates with TgGAP45 (Figs. 5, S3). Nevertheless, the non-palmitoylated protein continues to localize at the parasite periphery (Figs. 3, S1) and the motility of parasites expressing the mutant protein is in most aspects indistinguishable from wild-type parasites (Fig. 6).

How does palmitoylation of C8 and C11 affect the ability of TgMLC1 to bind TgGAP45? The detailed mechanism by which the N-terminus of TgMLC1 binds to the C-terminus of TgGAP45 (23) is unknown. Direct protein-protein interaction may be involved, as the mutation of two other sets of conserved N-terminal amino acids in TgMLC1 (D26E28 and P36GF38) also interfere with binding to TgGAP45 (23). The presence of the palmitates on C8 and C11 of TgMLC1 might help the interacting N-terminal residues of TgMLC1 transition from a disordered state (13, 20) into a binding-competent configuration. Alternatively, by inserting into the IMC membrane, the acyl chains could position the relevant N-terminal residues of TgMLC1 favorably for interaction with the C-terminus of TgGAP45, which is itself attached to the IMC membrane via palmitoylation. It is also possible that the acyl chains on TgMLC1 and TgGAP45 themselves interact within the plane of the membrane (20). In any of these cases, blocking TgMLC1 palmitoylation would be expected to inhibit TgMLC1-TgGAP45 interaction, as observed. It is unlikely that palmitoylation is necessary for proper folding and stability of TgMLC1, as appears

281 to be the case with the *P. falciparum* MLC1 homolog, MTIP (51), since (a) we see no evidence
282 for increased degradation of the C(8,11)S mutant compared to WT TgMLC1 (Fig. S4) and (b)
283 the palmitoylation-deficient mutants continue to bind to TgMyoA (*e.g.*, Fig 5).

284 Our data argue against the model that binding to TgGAP45 is what localizes TgMLC1 (and,
285 therefore, TgMyoA) to the parasite periphery and anchors the motor in the IMC membrane. We
286 showed that palmitoylation-deficient TgMLC1 no longer interacts with TgGAP45, yet both
287 TgMLC1 (Figs. 3, S1) and TgMyoA (Fig. S5) continue to localize to the periphery in these
288 mutant parasites. Previous studies with parasites expressing mutant TgGAP45 also argue against
289 a model in which the localization of TgMLC1 is determined by TgGAP45: TgGAP45 lacking its
290 C-terminal palmitoylation sites becomes dissociated from the IMC, yet TgMLC1 nevertheless
291 remained IMC associated (23). It is not clear how palmitoylated TgMLC1 located within the
292 space between the IMC and plasma membrane would be targeted to the IMC rather than the
293 plasma membrane, if not through TgGAP45. The simplest hypothesis is that it interacts directly
294 with one of the other resident proteins of the IMC, such as the transmembrane proteins
295 TgGAP40 or TgGAP50. Alternatively, insertion of TgMLC1 into the IMC could be a direct
296 consequence of binding to (63) and/or palmitoylation by IMC-localized palmitoyl S-acyl
297 transferases (61, 62).

298 The most unexpected result of this study was that the motility of parasites expressing C(8,11)S
299 TgMLC1 was in most aspects indistinguishable from wild-type parasites (Fig. 6). This
300 observation suggests that the coupling of the motor complex to the IMC via TgGAP45 is
301 unnecessary for force generation by the parasite, and directly contradicts a fundamental tenet of
302 the linear motor model of motility. The near normal motility observed in the mutants does not
303 appear to be due to compensatory changes in glideosome composition in response to the

304 mutations (*i.e.*, TgGAP45 does not associate with alternative myosin light chain(s) or myosin
305 motor(s) in the C[8,11]S mutant, nor does the mutant TgMLC1 or TgMyoA interact with
306 alternative GAP proteins; Fig. 7). It remains formally possible that non-palmitoylatable TgMLC1
307 binds to TgGAP45 in the parasite, with a reduced affinity that is sufficient to maintain its
308 association with the IMC and support motility but insufficient to survive detergent extraction and
309 immunoprecipitation. While it is difficult to experimentally exclude this possibility, most
310 previous studies of glideosome composition and function have utilized a similar nonionic
311 detergent extraction/immunoprecipitation approach, which constitutes the operational definition
312 of the glideosome (17, 18, 23). Furthermore, our phase partitioning experiments independently
313 suggest that the mutant TgMLC1 has indeed lost its association with the IMC membrane.
314 Finally, recent data demonstrate that parasites lacking TgMLC1 altogether have a defect in
315 motility initiation, but those parasites that continue to move do so at normal speeds (25).

316 At a minimum, our data demonstrate that TgMLC1 palmitoylation affects its binding to
317 TgGAP45 but this palmitoylation plays little to no role in parasite motility, as assayed by the
318 most sensitive and quantitative assays currently available. The data also show clearly that the
319 inhibitory effects of the palmitoylation inhibitor 2-bromopalmitate on parasite motility are not
320 due to changes in palmitoylation of TgMLC1, as previously hypothesized, although changes in
321 the palmitoylation of other glideosome components could be involved (64). While the data
322 presented here do not, by themselves, disprove the linear motor model of motility, they add to a
323 growing list of evidence (24-29, 33) suggesting that the mechanisms underlying apicomplexan
324 parasite motility are more complicated than what is currently encapsulated by the linear motor
325 model. How the different motility-associated proteins of the parasite interact and work together

to generate the forces necessary to drive parasite movement and whether more than one underlying mechanism exists remain important open questions for future study.

Materials and Methods

Parasite culture

T. gondii tachyzoites were maintained by serial passage in confluent monolayers of human foreskin fibroblasts (HFFs) (ATCC CRL-1634) grown in Dulbecco's Modified Eagle's Medium (DMEM), supplemented with 10% (v/v) heat-inactivated fetal bovine serum (FBS) and 10 mM HEPES, pH 7.0, as previously described (65). The medium was changed to DMEM supplemented with 1% (v/v) heat-inactivated FBS and 10 mM HEPES pH 7.0 prior to infection of confluent HFFs with parasites.

Generation of TgMLC1 knock-in mutants by allelic replacement

Mutations were introduced into a previously described *TgMLC1* allelic replacement plasmid (55) using the Quick Change site-directed mutagenesis kit (Agilent Technologies). *E.coli* were transformed with the mutagenized plasmids and colonies screened by colony PCR and restriction digestion. The entire open reading frame was sequenced to confirm the presence of only the desired mutation(s). The allelic replacement plasmid was linearized with BglII and PciI and used to transfect RHΔ*ku80*Δ*HXGPRT* parasites. Successful integration of the mutated gene at the endogenous locus yields phleomycin-resistant, FLAG-positive parasites. Parasites were therefore subjected to two rounds of phleomycin selection, cloned by limiting dilution and characterized by anti-FLAG immunofluorescence and immunoblotting, as well as diagnostic PCR to confirm correct integration on the chromosome (see Fig. S1). Finally, the presence of the desired mutations in individual clones was confirmed by sequencing of genomic DNA.

348 **Labeling with 17- ODYA**

349 ODYA labeling was performed as described previously (54).

350 **Epitope tagging of the *TgMyoA* locus using CRISPR/Cas9**

351 To insert the coding sequence for a Ty epitope tag at the C-terminus of *TgMyoA*, we constructed
352 plasmid pU6-MyoA, which contains the *TgMyoA* targeting chiRNA under the U6 promoter and
353 *Cas9* under the *TUB1* promoter (66). First, we synthesized a dsDNA oligo encoding the
354 protospacer sequence used to direct Cas9 to the C-terminal region of *TgMyoA*. To fuse the
355 *TgMyoA* protospacer to the chiRNA of the pU6-universal plasmid, forward and reverse oligos
356 corresponding to the *TgMyoA* 3' region were annealed by combining them (20µl each, 200µM
357 stocks) in duplex buffer (100mM potassium acetate; 30mM HEPES pH 7.5), heating them to
358 100°C for 2 minutes, then slowly cooling them to 25°C and letting them stand overnight to
359 generate double-stranded product. The duplexed oligos were dialyzed against deionized water,
360 phosphorylated using T4 polynucleotide kinase, and heat inactivated. Meanwhile, the pU6-
361 universal plasmid (5µg) was linearized by digesting with BsaI, dephosphorylated with Antarctic
362 phosphatase, heat inactivated and PCR purified. The phosphorylated, duplexed oligos were then
363 ligated into the pU6-universal plasmid to generate pU6-MyoAPS. Competent *E. coli* DH5-α
364 were transformed with the pU6-MyoAPS ligation mixture, and individual colonies with the
365 desired plasmid identified first by colony PCR, then by diagnostic PCR and sequencing. pU6-
366 MyoAPS was transfected along with duplexed, dialyzed homologous recombination (HR) oligos
367 into WT and C(8,11)S parasites. Ty-positive parasites were identified by immunofluorescence,
368 cloned by limiting dilution and confirmed as expressing TgMyoA-Ty from the endogenous

TgMyoA locus by immunofluorescence, diagnostic PCR (see Fig. S5), and sequencing of genomic DNA.

Immunofluorescence

HFF cells were infected for 15h and fixed with 4% (v/v) paraformaldehyde in PBS (15 min, 25°C). Fixed cells were washed and permeabilized with PBS containing 0.25% (v/v) Triton-X-100 for 20 minutes, washed 3 times with PBS and blocked (30 min, 25°C) in Block buffer (PBS containing 1% [w/v] BSA). The cells were then incubated for 1hr with primary antibodies diluted as follows with Block buffer: mouse monoclonal anti-FLAG (Sigma Aldrich) at 1:500; rabbit anti-GAP45 polyclonal serum (a generous gift from Dr. Con Beckers (17)) at 1:1000; rabbit anti-MyoA polyclonal serum (67) at 1:20; and rabbit anti-ELC1 polyclonal serum at 1:500. Samples were washed 3 times and incubated a further 30 min in goat-anti-rabbit IgG conjugated to Alexa fluor 546 (Invitrogen) or goat-anti-mouse IgG conjugated to Alexa fluor 488 (Invitrogen), each diluted 1:500 in Block buffer. After four final washes in PBS, fluorescence was visualized by epifluorescence microscopy.

Immunoprecipitation

For anti-FLAG immunoprecipitations, $2x10^7$ freshly egressed parasites were extracted for 45 minutes on ice in 3 ml of FLAG lysis buffer (10 mM imidazole pH 7.4, 300 mM NaCl, 1 mM EGTA, 5 mM $MgCl_2$, 1 % (w/v) TX-100, 2 mM DTT, 2mM ATP) containing 1:100 (v/v) protease inhibitors (Sigma #P8340). The extract was divided into two equal portions and insoluble material was pelleted at 10,000*xg* (30 min, 4°C). Each ~1.5 ml of supernatant was used to resuspend 20 ul of packed anti-FLAG M2 affinity resin (Sigma), then rocked gently overnight at 4°C. After three washes with the FLAG wash buffer (FLAG lysis buffer containing 1:500

(v/v) protease inhibitors), bound proteins from the pooled washed resin were eluted with 100µg of FLAG peptide (Sigma) in FLAG wash buffer. Eluates were resolved by SDS-PAGE and proteins visualized by immunoblotting. Primary and secondary (IRDye 680-conjugated anti-rabbit IgG and IRDye 800-conjugated anti-mouse IgG) antibodies were diluted for use in Odyssey blocking buffer (LI-COR). The blots were scanned using an Odyssey CLx infrared imager (LI-COR). Images were processed using Image Studio software (LI-COR). Signal intensities of bands being compared were normalized as described in the figure legends.

^{35}S-Metabolic labeling

For ^{35}S metabolic labeling, confluent HFF cells in a T75 flask were infected with $1x10^7$ tachyzoites and incubated for 16-20 hours. The infected cells were then incubated in methionine/cysteine-free DMEM (GIBCO) containing 1% (v/v) FBS for 1 hr, followed by 24 hr in DMEM containing 500µCi ^{35}S-Easytag mix (Perkin Elmer). Infected cells were detached from the flask using a cell scraper, washed twice with ice-cold PBS, and lysed in FLAG lysis buffer for anti-FLAG immunoprecipitation, or TX-100 lysis buffer (1% v/v TX-100, 50 mM Tris HCl pH 8.0, 150 mM NaCl, 2 mM EDTA and 1:200 (v/v) protease inhibitors) for anti-Ty and anti-GAP45 immunoprecipitations. Immunoprecipitation was performed as described above except that, after incubation with primary antibody, protein A-Sepharose (Invitrogen) was added and incubated for 1hr with gentle agitation at 4°C to collect the immune complexes. After three washes with either FLAG wash buffer or TX-100 IP wash buffer (1% v/v TX-100, 50 mM Tris, pH 8.0, 150 mM NaCl, 5 mM EDTA and 1:500 protease inhibitors), bound proteins were eluted in SDS-PAGE sample buffer by boiling at 100°C for 5 minutes. Samples were then resolved by SDS-PAGE, and transferred to PVDF membranes for phosphorimaging and immunoblotting.

Phase separation of parasite proteins in Triton X-114

The phase separation was performed as previously described (56-58). Briefly, $4x10^8$ tachyzoites were extracted in 1 ml extraction buffer (10 mM Tris-HCl, pH 7.4, 150 mM NaCl, 0.5% (v/v) precondensed TX-114 (Pierce) and 1:100 [v/v] dilution of protease inhibitors) for 90 minutes on ice. Insoluble material was removed by centrifugation (twice at 13,000x*g* for 5 min at 4°C). The cleared extract was overlaid onto a 750 µl prechilled sucrose cushion (6% [w/v] sucrose, 10 mM Tris-HCl, pH 7.4, 150 mM NaCl and 0.06% [v/v] precondensed Triton X-114), incubated for 5 minutes at 37°C and centrifuged to separate the detergent and aqueous phases by centrifugation (37°C, 3000x*g*, 5 min). Partitioning was repeated once on each phase and the collected samples were resolved by SDS-PAGE and analyzed by sequential incubations of a single western blot with anti-TgMyoA, -TgGAP45, -TgMLC1 and -TgELC1, followed by the appropriate secondary antibodies.

Motility assays

3D motility assays in Matrigel were performed as previously described (55, 68).

Protein identification by mass spectrometry analysis

Dried tryptic peptides recovered from excised gel bands (69) were dissolved in 10 µl 0.1% formic acid and 2.5% acetonitrile, and 2 ul were analyzed on the Thermo Q-Exactive mass spectrometer coupled to an EASY-nLC system (Thermo Fisher). Peptides were separated on a fused silica capillary (12 cm x 100 um I.D) packed with Halo C18 (2.7 um particle size, 90 nm pore size, Michrom Bioresources) at a flow rate of 300 nl/min. Peptides were introduced into the mass spectrometer via a nanospray ionization source at a spray voltage of 2.2 kV. Mass

spectrometry data were acquired in a data-dependent top-10 mode, and the lock mass function was activated (m/z, 371.1012). Full scans were acquired from m/z 350 to 1,600 at 70,000 resolution (automatic gain control [AGC] target, 1e6; maximum ion time [max IT], 100 ms; profile mode). Resolution for dd-MS^2 spectra was set to 17,500 (AGC target: 1e5) with a maximum ion injection time of 50 ms. The normalized collision energy was 27 eV. A gradient of 0 to 40% acetonitrile (0.1% FA) over 55 min was applied. The spectra were searched against the *T. gondii* protein database (http://www.toxodb.org/toxo/) by Proteome Discoverer (PD) 2.0. The search parameters permitted a 10 ppm precursor MS tolerance and a 0.02 Da MS/MS tolerance. Carboxymethylation of cysteines was set up as fixed modification and Oxidation of methionine (M) was allowed as variable modification. Up to three missed tryptic cleavages of peptides were considered with the false-discovery rate set to 1% at the peptide level.

Figure and Table Legends

Figure 1. Schematic illustrations of the glideosome and TgMLC1 domain structure. (A) In the linear motor model of motility (reviewed in (16)), the TgMyoA motor (TgMyoA and its associated light chains, TgMLC1 and either TgELC1 or TgELC2) is anchored to the parasite's inner membrane complex (IMC) via the acylated glideosome-associated protein, TgGAP45, and the transmembrane proteins TgGAP40 and TgGAP50. The lumenal portion of GAP50 is thought to interact with GAPM, a protein that spans the inner IMC membrane, and which likely connects the entire glideoeome to the underlying parasite cytoskeleton. Short actin (TgACT1) filaments located between the parasite plasma membrane and the IMC are connected to ligands on the substrate through a linker protein, possibly the glideosome-associated connector protein (GAC), which binds to the cytosolic tails of surface adhesins such as TgMIC2. The TgMyoA motor

456 displaces the actin filaments rearward; because the motor is connected to the IMC and the actin
457 is connected to the substrate, this causes the parasite to move forward relative to the substrate.
458 The depiction of a pair of acyl chains on the N-terminus of TgMLC1 (red squiggles) and their
459 interaction with the IMC membrane is based on results reported here. **(B)** TgMLC1 consists of a
460 44-amino acid N-terminal extension, a central disordered region, and four EF hand-like domains,
461 which interact with the tail of TgMyoA. The positions of the five cysteines in the protein are
462 shown in blue; CSS-Palm 4.0 predicted C8 and C11 as likely sites of palmitoylation.

463 **Figure 2. Cys8 and Cys11 are the likely sites of palmitoylation on TgMLC1.** Parasites
464 expressing either wild-type (WT) or mutant FLAG-tagged TgMLC1 were labeled with the
465 palmitic acid analog 17-ODYA, and anti-FLAG resin was then used to pull down FLAG-
466 TgMLC1 and associated proteins. The proteins in the pulldown were resolved by SDS-PAGE
467 and visualized either by rhodamine fluorescence scan (upper panel), to show the position of 17-
468 ODYA in the gel, or by western blotting with anti-TgMLC1 (lower panel). Numbers on the left
469 indicate molecular mass in kDa; only the ~30kDa portion of the western blot is shown. The
470 predominant ~31-kDa ODYA-labeled band comigrates with FLAG-TgMLC1; its labeling
471 intensity is reduced in the C8S and C11S single mutants and abolished completely in the
472 C(8,11)S and C(8,11)A double mutants. The western blot shows similar protein loads in all
473 samples. The asterisk indicates a doublet of ODYA-labeled proteins at ~50kDa that is pulled
474 down with wild-type FLAG-TgMLC1 but not with either of the double mutants – see text for
475 details.

476 **Figure 3. C(8,11)S and C(8,11)A mutations do not affect localization of TgMLC1 to the**
477 **parasite periphery.** Infected HFF cells were fixed, permeabilized and stained for FLAG-tagged
478 TgMLC1 (red) or TgGAP45 (green). The corresponding merged and DIC images are also

shown. Upper panels compare the localization of WT *vs*. C(8,11)S TgMLC1; lower panels compare WT *vs.* C(8,11)A TgMLC1. Scale bar = 10 μm.

Figure 4. Blocking TgMLC1 palmitoylation causes the protein to shift into the aqueous phase in Triton X-114. WT, C8S, C11S, C(8,11)S and C(8,11)A parasites were extracted at 4°C in Triton X-114 and the extracted proteins phase partitioned by shifting the temperature to 20°C. The amounts of **(A)** TgMLC1and **(B)** TgGRA8 recovered in the detergent (grey) and aqueous (black) phases from each sample were determined by quantitative western blotting (see Fig. S2 for a representative western blot), and are displayed here as the percentage of the total TgMLC1 recovered in the two phases combined. The data shown are the means and standard error of the mean (SEM) from 2 (C8S, C11S) or 4 (WT, C[8,11]S) independent replicates; C(8,11)A parasites were analyzed once.

Figure 5. Blocking TgMLC1 palmitoylation alters the composition of the glideosome. (A) Parasites expressing wild-type or mutant FLAG-tagged TgMLC1 were gently extracted in Triton X-100, and the soluble proteins (Input) were used for anti-FLAG immunoprecipitations (FLAG IP). Immunoprecipitated proteins were resolved by SDS-PAGE and analyzed by sequential western blotting with anti-TgMyoA, -TgGAP45, -TgMLC1 and -TgELC1; the fluorescent signal intensity of each immunoreactive band is indicated by the white number below the band (relative fluorescence units). Numbers on the left indicate molecular mass in kDa. **(B)** The signal intensities of TgGAP45, TgMyoA and TgELC1 immunoprecipitated from the C(8,11)S mutant parasite line is shown relative the corresponding band from the WT line, after normalizing to the amount of TgMLC1 recovered in each sample. Shown are the means and SEM from six independent experiments; differences were assessed using an unpaired two-tailed t-test.

Figure 6. Mutations that block TgMLC1 palmitoylation and disrupt glideosome composition have little effect on parasite motility. The upper panels show maximum intensity projections of the Hoechst 33342-stained WT or C[8,11]S parasites that moved within a 3-dimensional model extracellular matrix (Matrigel) during 60 sec of image capture. Scale bar = 50 µm. The table below shows the motility parameters calculated from three independent motility assays (each consisting of three technical replicates); numbers for each parameter represent the means +/- SEM. The total number of trajectories analyzed for each parasite line is also shown. Differences between WT and C(8,11)S parasites for each motility parameter were assessed using an unpaired two-tailed t-test and the resulting *p* values are shown in the righthand column.

Figure 7. No changes in glideosome composition that could compensate for the loss of TgGAP45-TgMLC1 interaction are observed in C(8,11)S parasites. Parasites were labeled for 24 hr in medium containing (^{35}S)- methionine/cysteine and gently extracted in Triton X-100. Soluble proteins were immunoprecipitated as described below, resolved by SDS-PAGE, transferred to a PVDF membrane and visualized by phosphorimaging (shown here). The same membrane was subsequently used for western blotting, probing with antibodies against TgMyoA, TgGAP45 and TgMLC1 (not shown) to determine which ^{35}S-labeled bands corresponded to which glideosome proteins. Numbers on the left of each panel indicate molecular mass in kDa. **(A)** To test whether TgGAP45 interacts with any new proteins in C(8,11)S parasites, ^{35}S-labeled proteins from WT and C(8,11)S parasites were immunoprecipitated with anti-TgGAP45, resolved by SDS/PAGE and visualized by phosphorimaging. No bands were detected in the pulldowns from C(8,11)S parasites that were not already present in the pulldowns from WT parasites. The band migrating immediately below TgGAP45 in the WT sample was recovered in some pulldowns but not others and may represent

a breakdown product of TgGAPA45 (see Fig. S7). **(B)** To test whether TgMyoA interacts with any new proteins in the C(8,11)S parasites, ^{35}S-labeled proteins immunoprecipitated using anti-Ty from WT-MyoATy and C(8,11)S-MyoATy parasites were compared. No bands were detected in the pulldowns from C(8,11)S parasites that were not already present in the pulldowns from WT parasites. **(C)** To test whether C(8,11)S TgMLC1 interacts with any new proteins compared to WT TgMLC1, ^{35}S-labeled proteins immunoprecipitated using anti-FLAG from WT and C(8,11)S parasites were compared. Asterisk indicates an ~80K band enriched in the FLAG pulldown of C(8,11)S compared to WT; this protein was shown to be a fragment of TgMyoA (see text). The relative amounts of TgMyoA and TgGAP45 pulled down in Panel C were quantified by western blotting as shown in Fig. S6.

Table 1: Strains generated and used in this study, with their relevant genotypes

Supplementary figure legends and tables

Figure S1. Generation and characterization of TgMLC1 knock-in parasites. (A) Allelic replacement strategy. The *TgMLC1* allele was targeted in *RHΔku80* parasites using 5' and 3' *TgMLC1* homology regions flanking a construct that consisted of cDNA encoding full-length TgMLC1 (wildtype or mutant) with an N-terminal FLAG tag, the *3'* untranslated region (UTR) from *DHFR,* and a selection cassette consisting of the *GRA1* promoter, the phleomycin resistance gene (*ble*) and the 3' UTR from *SAG1.* The binding location of PCR primers P1-P4 (which correspond to Primers 25-28, respectively, in Supplementary Table 11) and the corresponding expected amplicon sizes are indicated in red. This same strategy was used to generate all TgMLC1 knock-in lines. Panels B-D illustrate how insertion at the genomic locus and correct localization and expression of the mutant protein was confirmed in each knock-in

line; results for the C(8,11)S parasite line are shown here. **(B)** PCR results using primer pairs P1+P2 and P3+P4 on parental (*Δku80)* and C(8,11)S parasites after allelic replacement. DNA ladder is shown in the leftmost lane, numbers indicate base pairs. **(C)** Immunofluorescence staining of C(8,11)S parasites with anti-GAP45 (red) and anti-FLAG (green) confirms expression and proper (peripheral) localization of the FLAG-tagged TgMLC1. Scale bar = 10 µm. **(D)** Western blot of C(8,11)S parasites stained with anti TgMyoA (green) and anti-FLAG (red) confirms expression and proper size of the FLAG-tagged protein. Numbers on the left indicate molecular mass in kDa. Successful allelic replacement by constructs expressing WT, C8S, C11S and C8A11A TgMLC1 were similarly confirmed by PCR, immunofluorescence and western blot.

Figure S2. Triton X-114 phase partitioning of parasites expressing WT *vs.* palmitoylation-deficient TgMLC1. WT, C8S, C11S and C8SC11S parasites were extracted at 4°C in Triton X-114 and subjected to phase partitioning at 20°C. Proteins present in the lysate before partitioning (Whole lysate) and in the aqueous and detergent phases after partitioning were resolved by SDS-PAGE and visualized either by **(A)** Western blotting with anti-TgMLC1 (green) and anti-TgGRA8 (red), or **(B)** Colloidal Coomassie staining. Numbers on the left of each panel indicate molecular mass in kDa.

Figure S3. Similar changes in the composition of the glideosome are observed in C(8,11)S and C(8,11)A parasites. (A) Parasites expressing wild-type or mutant FLAG-tagged TgMLC1 were gently extracted in Triton X-100, and the soluble proteins (Input) used for anti-FLAG immunoprecipitations. Proteins that bound to the anti-FLAG affinity resin and those that did not (Bound, Unbound) were recovered and analyzed by SDS-PAGE and sequential western blotting

with anti-TgMyoA, -TgGAP45, -TgMLC1 and -TgELC1. The signal intensity of each immunoreactive band was quantified (white number below the band; relative fluorescence units). Numbers on the left indicate molecular mass in kDa. **(B)** The signal intensities of TgGAP45, TgMyoA and TgELC1 pulled down from each of the parasite lines is shown relative the corresponding band from WT parasites, after normalizing to the amount of TgMLC1 recovered in each sample. Shown are the means and SEM from three independent experiments; data were analyzed using one-way ANOVA.

Figure S4. WT, C(8,11)S and C(8,11)A parasites express equivalent amounts of both FLAG-tagged TgMLC1 and TgMyoA. Parasite proteins were extracted in boiling SDS-PAGE sample buffer, resolved by SDS-PAGE and visualized by western blotting with anti-TgMyoA and anti-TgMLC1 (left panel) or anti-TgIMC1 (right panel) as a loading control. The signal intensity of each immunoreactive band was quantified (white number below the band; relative fluorescence units). Numbers on the left indicate molecular mass in kDa. **(B)** The signal intensities of TgMyoA and TgMLC1 in each of the parasite lines is shown relative the corresponding band from wildtype parasites, after normalizing to the amount of TgIMC1 in each sample.

Figure S5. Generation and characterization of parasites expressing C-terminally Ty-tagged TgMyoA. (A) Schematic representation of the *TgMyoA* locus after the insertion of Ty tag at the 3' end using CRISPR-Cas9. The binding location of PCR primers P1-P3 and the expected amplicon sizes are indicated. Primers P1, P2 and P3 correspond to primers 20, 22 and 21, respectively, in Supplementary Table 11. **(B)** PCR results using primer pairs P1+P2 and P1+P3 on parental parasites (*Δku80)* and the WT and C(8,11)S lines after Ty tagging the *TgMyoA* locus.

DNA ladder is shown in the leftmost lane, numbers indicate base pairs. **(C)** Immunofluorescence staining of WT-MyoATy and C(8,11)S-MyoATy parasites with anti-Ty (red) and anti-GAP45 (green) confirms expression and proper localization of Ty-tagged TgMyoA in the two lines. Scale bar = 10 μm. **(D)** Western blots of WT-MyoATy and C(8,11)S-MyoATy parasites probed with anti-Ty (red) followed by anti-TgMyoA and TgMLC1 (green) confirms similar expression levels of TgMyoA in the two lines. Numbers on the left indicate molecular mass in kDa.

Figure S6: The western blot signal intensities of **(A)** TgMyoA and **(B)** TgGAP45 pulled down from WT or C(8,11)S parasites in Fig. 7C, after normalizing for the amount of TgMLC1 recovered in each sample. Shown are the means and SEM from two independent experiments; differences were assessed using an unpaired two-tailed t-test.

Figure S7. Preparative SDS-PAGE of anti-FLAG immunoprecipitated proteins from WT and C(8,11)S parasites. Proteins immunoprecipitated using anti-FLAG from WT and C(8,11)S parasites were resolved by SDS-PAGE and stained with colloidal Coomassie Blue. The major stained bands were excised, digested with trypsin and identified by LC/MS-MS as described in Materials and Methods. Numbers on the left indicate molecular mass in kDa. Labels on the right indicate the major protein identified in the band and the LC/MS-MS data file on which this identification was based (see Table S1 for a summary of the LC/MS-MS results and Tables S2-S10 for the raw data for each band).

Supplementary Tables 1-10: Identification of protein bands recovered in the anti-FLAG immunoprecipitates from WT and C(8,11)S parasites. Protein identification data for the nine excised bands shown in Fig. S6 are summarized in Table S1, and the raw LC/MS-MS results for each individual band are provided in Tables S2-S10.

612 **Supplementary Table 11. List of oligonucleotides used in this study**

613 Acknowledgements

614 This work was supported by US Public Health Service grants AI139201 to GEW and GM111703
615 to MB. The Vermont Genetics Network Proteomics Facility is supported through NIH grant
616 P20GM103449 from the INBRE Program of the National Institute of General Medical Sciences.
617 The funders had no role in study design, data collection and interpretation, or the decision to
618 submit the work for publication.

619 References

620 1. Montoya JG, Liesenfeld O. 2004. Toxoplasmosis. Lancet 363:1965-76.

621 2. Barragan A, Sibley LD. 2002. Transepithelial migration of Toxoplasma gondii is linked to
622 parasite motility and virulence. J Exp Med 195:1625-33.

623 3. Harker KS, Ueno N, Lodoen MB. 2015. *Toxoplasma gondii* Dissemination: A Parasite's
624 Journey through the Infected Host. Parasite Immunol 37:141-149.

625 4. Sibley LD. 2004. Intracellular parasite invasion strategies. Science 304:248-53.

626 5. Heintzelman MB, Schwartzman JD. 1997. A novel class of unconventional myosins from
627 *Toxoplasma gondii*. J Mol Biol 271:139-46.

628 6. Pinder JC, Fowler RE, Dluzewski AR, Bannister LH, Lavin FM, Mitchell GH, Wilson RJ,
629 Gratzer WB. 1998. Actomyosin motor in the merozoite of the malaria parasite, Plasmodium
630 falciparum: implications for red cell invasion. J Cell Sci 111 (Pt 13):1831-9.

631 7. Herm-Gotz A, Weiss S, Stratmann R, Fujita-Becker S, Ruff C, Meyhofer E, Soldati T,
632 Manstein DJ, Geeves MA, Soldati D. 2002. Toxoplasma gondii myosin A and its light chain:
633 a fast, single-headed, plus-end-directed motor. EMBO J 21:2149-58.

634 8. Baum J, Richard D, Healer J, Rug M, Krnajski Z, Gilberger TW, Green JL, Holder AA,
635 Cowman AF. 2006. A conserved molecular motor drives cell invasion and gliding motility
636 across malaria life cycle stages and other apicomplexan parasites. J Biol Chem 281:5197-208.

637 9. Nebl T, Prieto JH, Kapp E, Smith BJ, Williams MJ, Yates JR, 3rd, Cowman AF, Tonkin CJ.
638 2011. Quantitative in vivo analyses reveal calcium-dependent phosphorylation sites and
639 identifies a novel component of the Toxoplasma invasion motor complex. PLoS Pathog
640 7:e1002222.

641 10. Bookwalter CS, Kelsen A, Leung JM, Ward GE, Trybus KM. 2014. A Toxoplasma gondii
642 class XIV myosin, expressed in Sf9 cells with a parasite co-chaperone, requires two light
643 chains for fast motility. J Biol Chem 289:30832-41.

644 11. Williams MJ, Alonso H, Enciso M, Egarter S, Sheiner L, Meissner M, Striepen B, Smith BJ,
645 Tonkin CJ. 2015. Two Essential Light Chains Regulate the MyoA Lever Arm To Promote
646 *Toxoplasma* Gliding Motility. MBio 6:e00845-15.

647 12. Green JL, Wall RJ, Vahokoski J, Yusuf NA, Ridzuan MAM, Stanway RR, Stock J, Knuepfer
648 E, Brady D, Martin SR, Howell SA, Pires IP, Moon RW, Molloy JE, Kursula I, Tewari R,
649 Holder AA. 2017. Compositional and expression analyses of the glideosome during the
650 Plasmodium life cycle reveal an additional myosin light chain required for maximum motility.
651 J Biol Chem 292:17857-17875.

652 13. Powell CJ, Jenkins ML, Parker ML, Ramaswamy R, Kelsen A, Warshaw DM, Ward GE,
653 Burke JE, Boulanger MJ. 2017. Dissecting the molecular assembly of the *Toxoplasma gondii*
654 MyoA motility complex. J Biol Chem 292:19469-19477.

655 14. Powell CJ, Ramaswamy R, Kelsen A, Hamelin DJ, Warshaw DM, Bosch J, Burke JE, Ward
656 GE, Boulanger MJ. 2018. Structural and mechanistic insights into the function of the
657 unconventional class XIV myosin MyoA from Toxoplasma gondii. Proc Natl Acad Sci U S A
658 115:E10548-e10555.

659 15. Robert-Paganin J, Robblee JP, Auguin D, Blake TCA, Bookwalter CS, Krementsova EB,
660 Moussaoui D, Previs MJ, Jousset G, Baum J, Trybus KM, Houdusse A. 2019. Plasmodium
661 myosin A drives parasite invasion by an atypical force generating mechanism. Nat Commun
662 10:3286.

663 16. Frenal K, Dubremetz JF, Lebrun M, Soldati-Favre D. 2017. Gliding motility powers invasion
664 and egress in Apicomplexa. Nat Rev Microbiol 15:645-660.

17. Gaskins E, Gilk S, DeVore N, Mann T, Ward G, Beckers C. 2004. Identification of the membrane receptor of a class XIV myosin in Toxoplasma gondii. J Cell Biol 165:383-93.

18. Johnson TM, Rajfur Z, Jacobson K, Beckers CJ. 2007. Immobilization of the Type XIV Myosin Complex in *Toxoplasma gondii*. Mol Biol Cell 18:3039-3046.

19. Jacot D, Tosetti N, Pires I, Stock J, Graindorge A, Hung YF, Han H, Tewari R, Kursula I, Soldati-Favre D. 2016. An Apicomplexan Actin-Binding Protein Serves as a Connector and Lipid Sensor to Coordinate Motility and Invasion. Cell Host Microbe 20:731-743.

20. Pazicky S, Dhamotharan K, Kaszuba K, Mertens H, Gilberger T, Svergun D, Kosinski J, Weininger U, Löw C. 2019. Structural role of essential light chains in the apicomplexan glideosome. bioRxiv doi:10.1101/867499:867499.

21. Warshaw DM. 2004. Lever arms and necks: a common mechanistic theme across the myosin superfamily. J Muscle Res Cell Motil 25:467-74.

22. Bergman LW, Kaiser K, Fujioka H, Coppens I, Daly TM, Fox S, Matuschewski K, Nussenzweig V, Kappe SH. 2003. Myosin A tail domain interacting protein (MTIP) localizes to the inner membrane complex of *Plasmodium* sporozoites. J Cell Sci 116:39-49.

23. Frenal K, Polonais V, Marq JB, Stratmann R, Limenitakis J, Soldati-Favre D. 2010. Functional dissection of the apicomplexan glideosome molecular architecture. Cell Host Microbe 8:343-57.

24. Egarter S, Andenmatten N, Jackson AJ, Whitelaw JA, Pall G, Black JA, Ferguson DJ, Tardieux I, Mogilner A, Meissner M. 2014. The toxoplasma Acto-MyoA motor complex is important but not essential for gliding motility and host cell invasion. PLoS One 9:e91819.

25. Whitelaw JA, Latorre-Barragan F, Gras S, Pall GS, Leung JM, Heaslip A, Egarter S, Andenmatten N, Nelson SR, Warshaw DM, Ward GE, Meissner M. 2017. Surface attachment, promoted by the actomyosin system of *Toxoplasma gondii* is important for efficient gliding motility and invasion. BMC Biol 15:1.

26. Andenmatten N, Egarter S, Jackson AJ, Jullien N, Herman JP, Meissner M. 2013. Conditional genome engineering in Toxoplasma gondii uncovers alternative invasion mechanisms. Nat Methods 10:125-7.

693 27. Meissner M, Ferguson DJ, Frischknecht F. 2013. Invasion factors of apicomplexan parasites:
694 essential or redundant? Curr Opin Microbiol 16:438-44.

695 28. Pavlou G, Touquet B, Vigetti L, Renesto P, Bougdour A, Debarre D, Balland M, Tardieux I.
696 2020. Coupling Polar Adhesion with Traction, Spring and Torque Forces Allows High Speed
697 Helical Migration of the Protozoan Parasite Toxoplasma. ACS Nano 14:7121-7139.

698 29. Tardieux I, Baum J. 2016. Reassessing the mechanics of parasite motility and host-cell
699 invasion. J Cell Biol 214:507-15.

700 30. Bane KS, Lepper S, Kehrer J, Sattler JM, Singer M, Reinig M, Klug D, Heiss K, Baum J,
701 Mueller AK, Frischknecht F. 2016. The Actin Filament-Binding Protein Coronin Regulates
702 Motility in Plasmodium Sporozoites. PLoS Pathog 12:e1005710.

703 31. Kappe S, Bruderer T, Gantt S, Fujioka H, Nussenzweig V, Menard R. 1999. Conservation of
704 a gliding motility and cell invasion machinery in apicomplexan parasites. J Cell Biol 147:937-
705 44.

706 32. Munter S, Sabass B, Selhuber-Unkel C, Kudryashev M, Hegge S, Engel U, Spatz JP,
707 Matuschewski K, Schwarz US, Frischknecht F. 2009. *Plasmodium* sporozoite motility is
708 modulated by the turnover of discrete adhesion sites. Cell Host Microbe 6:551-62.

709 33. Quadt KA, Streichfuss M, Moreau CA, Spatz JP, Frischknecht F. 2016. Coupling of
710 Retrograde Flow to Force Production During Malaria Parasite Migration. ACS Nano 10:2091-
711 102.

712 34. Carey KL, Westwood NJ, Mitchison TJ, Ward GE. 2004. A small-molecule approach to
713 studying invasive mechanisms of *Toxoplasma gondii*. Proc Natl Acad Sci U S A 101:7433-8.

714 35. Farrell A, Thirugnanam S, Lorestani A, Dvorin JD, Eidell KP, Ferguson DJ, Anderson-White
715 BR, Duraisingh MT, Marth GT, Gubbels MJ. 2012. A DOC2 protein identified by mutational
716 profiling is essential for apicomplexan parasite exocytosis. Science 335:218-21.

717 36. Hegge S, Münter S, Steinbüchel M, Heiss K, Engel U, Matuschewski K, Frischknecht F. 2010.
718 Multistep adhesion of Plasmodium sporozoites. Faseb J 24:2222-34.

719 37. Drewry LL, Sibley LD. 2015. *Toxoplasma* Actin Is Required for Efficient Host Cell Invasion.
720 MBio 6:e00557.

721 38. Linder ME, Deschenes RJ. 2007. Palmitoylation: policing protein stability and traffic. Nat Rev
722 Mol Cell Biol 8:74-84.

723 39. Tom CT, Martin BR. 2013. Fat chance! Getting a grip on a slippery modification. ACS Chem
724 Biol 8:46-57.

725 40. Linder ME, Deschenes RJ. 2003. New insights into the mechanisms of protein palmitoylation.
726 Biochemistry 42:4311-20.

727 41. Salaun C, Greaves J, Chamberlain LH. 2010. The intracellular dynamic of protein
728 palmitoylation. J Cell Biol 191:1229-38.

729 42. Resh MD. 2006. Palmitoylation of ligands, receptors, and intracellular signaling molecules.
730 Sci STKE 2006:re14.

731 43. Beck JR, Fung C, Straub KW, Coppens I, Vashisht AA, Wohlschlegel JA, Bradley PJ. 2013.
732 A Toxoplasma palmitoyl acyl transferase and the palmitoylated armadillo repeat protein
733 TgARO govern apical rhoptry tethering and reveal a critical role for the rhoptries in host cell
734 invasion but not egress. PLoS Pathog 9:e1003162.

735 44. Caballero MC, Alonso AM, Deng B, Attias M, de Souza W, Corvi MM. 2016. Identification
736 of new palmitoylated proteins in *Toxoplasma gondii*. Biochim Biophys Acta 1864:400-8.

737 45. Child MA, Hall CI, Beck JR, Ofori LO, Albrow VE, Garland M, Bowyer PW, Bradley PJ,
738 Powers JC, Boothroyd JC, Weerapana E, Bogyo M. 2013. Small-molecule inhibition of a
739 depalmitoylase enhances Toxoplasma host-cell invasion. Nat Chem Biol 9:651-6.

740 46. Corvi MM, Turowski VR. 2019. Palmitoylation in apicomplexan parasites: from established
741 regulatory roles to putative new functions. Mol Biochem Parasitol 230:16-23.

742 47. De Napoli MG, de Miguel N, Lebrun M, Moreno SN, Angel SO, Corvi MM. 2013. N-terminal
743 palmitoylation is required for Toxoplasma gondii HSP20 inner membrane complex
744 localization. Biochim Biophys Acta 1833:1329-37.

745 48. Frenal K, Kemp LE, Soldati-Favre D. 2014. Emerging roles for protein S-palmitoylation in
746 Toxoplasma biology. Int J Parasitol 44:121-31.

747 49. Fung C, Beck JR, Robertson SD, Gubbels MJ, Bradley PJ. 2012. *Toxoplasma* ISP4 is a central
748 IMC Sub-compartment Protein whose localization depends on palmitoylation but not
749 myristoylation. Mol Biochem Parasitol 184:99-108.

750 50. Hopp CS, Balaban AE, Bushell ES, Billker O, Rayner JC, Sinnis P. 2016. Palmitoyl
751 transferases have critical roles in the development of mosquito and liver stages of *Plasmodium*.
752 Cell Microbiol 18:1625-1641.

753 51. Jones ML, Collins MO, Goulding D, Choudhary JS, Rayner JC. 2012. Analysis of protein
754 palmitoylation reveals a pervasive role in Plasmodium development and pathogenesis. Cell
755 Host Microbe 12:246-58.

756 52. Tremp AZ, Al-Khattaf FS, Dessens JT. 2017. Palmitoylation of *Plasmodium* alveolins
757 promotes cytoskeletal function. Mol Biochem Parasitol 213:16-21.

758 53. Wetzel J, Herrmann S, Swapna LS, Prusty D, Peter AT, Kono M, Saini S, Nellimarla S, Wong
759 TW, Wilcke L, Ramsay O, Cabrera A, Biller L, Heincke D, Mossman K, Spielmann T,
760 Ungermann C, Parkinson J, Gilberger TW. 2014. The role of palmitoylation for protein
761 recruitment to the inner membrane complex of the malaria parasite. J Biol Chem 290:1712-28.

762 54. Foe IT, Child MA, Majmudar JD, Krishnamurthy S, van der Linden WA, Ward GE, Martin
763 BR, Bogyo M. 2015. Global Analysis of Palmitoylated Proteins in Toxoplasma gondii. Cell
764 Host Microbe 18:501-11.

765 55. Leung JM, Tran F, Pathak RB, Poupart S, Heaslip AT, Ballif BA, Westwood NJ, Ward GE.
766 2014. Identification of T. gondii myosin light chain-1 as a direct target of TachypleginA-2, a
767 small-molecule inhibitor of parasite motility and invasion. PLoS One 9:e98056.

768 56. Bordier C. 1981. Phase separation of integral membrane proteins in Triton X-114 solution. J
769 Biol Chem 256:1604-7.

770 57. Wichroski MJ, Ward GE. 2003. Biosynthesis of glycosylphosphatidylinositol is essential to
771 the survival of the protozoan parasite *Toxoplasma gondii*. Eukaryot Cell 2:1132-6.

772 58. Carey KL, Donahue CG, Ward GE. 2000. Identification and molecular characterization of
773 GRA8, a novel, proline-rich, dense granule protein of Toxoplasma gondii. Mol Biochem
774 Parasitol 105:25-37.

775 59. Frenal K, Marq JB, Jacot D, Polonais V, Soldati-Favre D. 2014. Plasticity between MyoC- and
776 MyoA-glideosomes: an example of functional compensation in Toxoplasma gondii invasion.
777 PLoS Pathog 10:e1004504.

778 60. Rees-Channer RR, Martin SR, Green JL, Bowyer PW, Grainger M, Molloy JE, Holder AA.
779 2006. Dual acylation of the 45 kDa gliding-associated protein (GAP45) in Plasmodium
780 falciparum merozoites. Mol Biochem Parasitol 149:113-6.

781 61. Frenal K, Tay CL, Mueller C, Bushell ES, Jia Y, Graindorge A, Billker O, Rayner JC, Soldati-
782 Favre D. 2013. Global analysis of apicomplexan protein S-acyl transferases reveals an enzyme
783 essential for invasion. Traffic 14:895-911.

784 62. Dogga SK, Frenal K. 2020. Two palmitoyl acyltransferases involved sequentially in the
785 biogenesis of the inner membrane complex of Toxoplasma gondii. Cell Microbiol April
786 23:e13212.

787 63. Thomas GM, Hayashi T, Chiu SL, Chen CM, Huganir RL. 2012. Palmitoylation by DHHC5/8
788 targets GRIP1 to dendritic endosomes to regulate AMPA-R trafficking. Neuron 73:482-96.

789 64. Alonso AM, Coceres VM, De Napoli MG, Nieto Guil AF, Angel SO, Corvi MM. 2012. Protein
790 palmitoylation inhibition by 2-bromopalmitate alters gliding, host cell invasion and parasite
791 morphology in Toxoplasma gondii. Mol Biochem Parasitol 184:39-43.

792 65. Roos DS. 1996. Molecular genetic tools for the identification and analysis of drug targets in
793 *Toxoplasma gondii*. Curr Top Microbiol Immunol 219:247-59.

794 66. Sidik SM, Hackett CG, Tran F, Westwood NJ, Lourido S. 2014. Efficient genome engineering
795 of Toxoplasma gondii using CRISPR/Cas9. PLoS One 9:e100450.

796 67. Tang Q, Andenmatten N, Hortua Triana MA, Deng B, Meissner M, Moreno SNJ, Ballif BA,
797 Ward GE. 2014. Calcium-dependent phosphorylation alters Class XIVa myosin function in the
798 protozoan parasite *Toxoplasma gondii*. Mol Biol Cell 25:2579-2791.

799 68. Leung JM, Rould MA, Konradt C, Hunter CA, Ward GE. 2014. Disruption of TgPHIL1 alters
800 specific parameters of Toxoplasma gondii motility measured in a quantitative, three-
801 dimensional live motility assay. PLoS One 9:e85763.

802 69. Krishnamurthy S, Deng B, Del Rio R, Buchholz KR, Treeck M, Urban S, Boothroyd J, Lam
803 YW, Ward GE. 2016. Not a Simple Tether: Binding of Toxoplasma gondii AMA1 to RON2
804 during Invasion Protects AMA1 from Rhomboid-Mediated Cleavage and Leads to
805 Dephosphorylation of Its Cytosolic Tail. MBio 7:e00754-16.

806

Figure 1

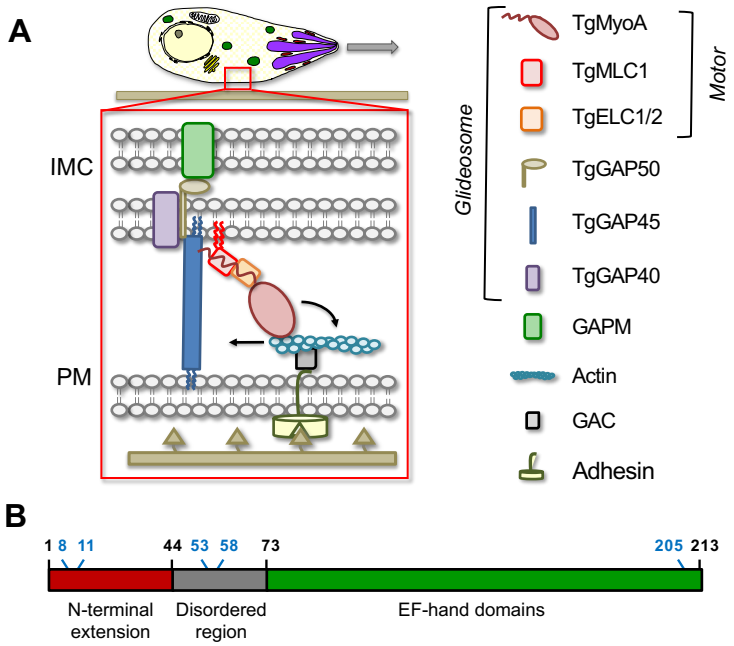

Figure 2

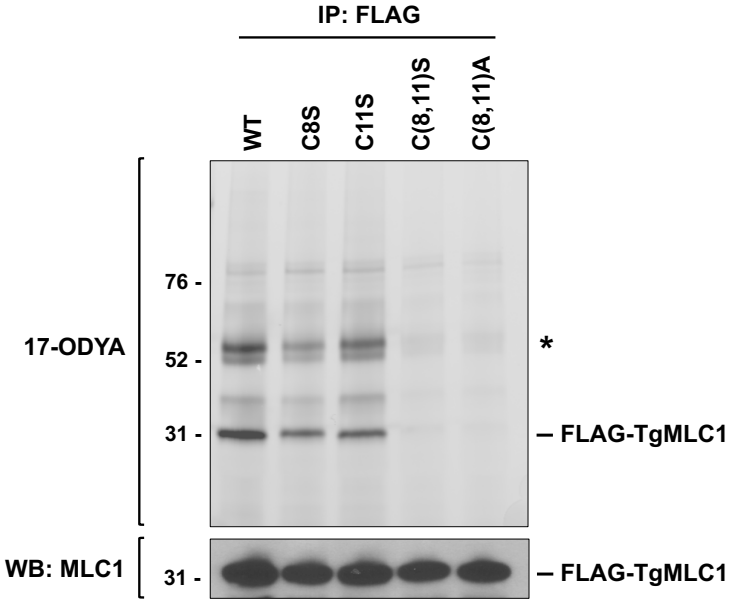

Figure 3

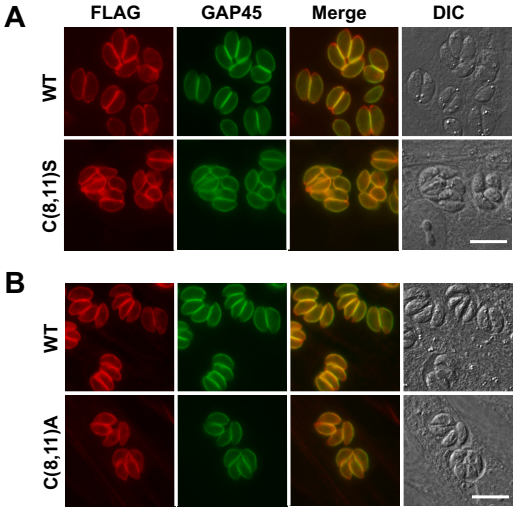

Figure 4

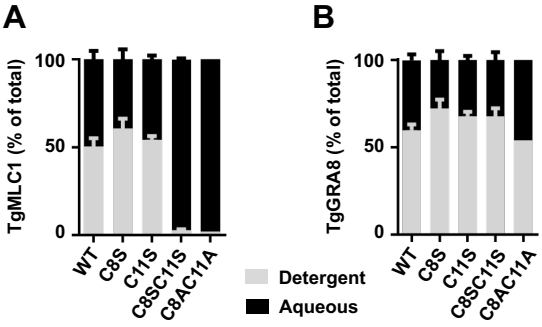

Figure 5

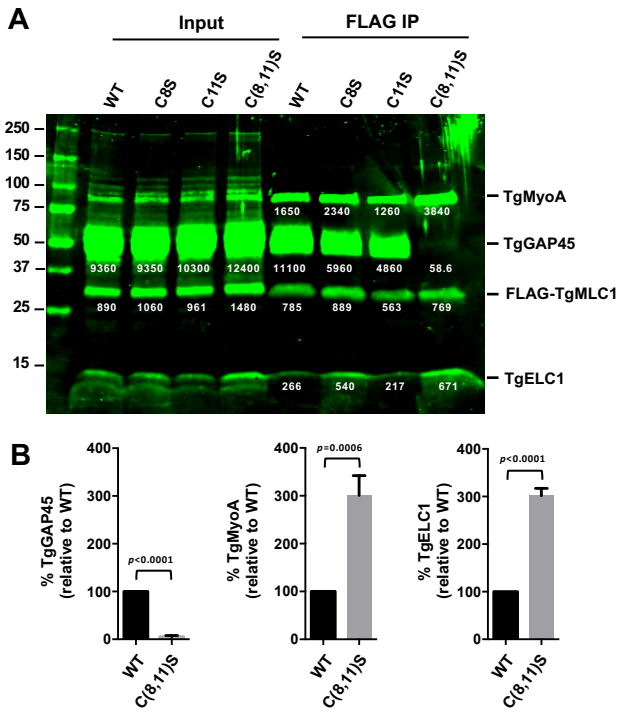

Figure 6

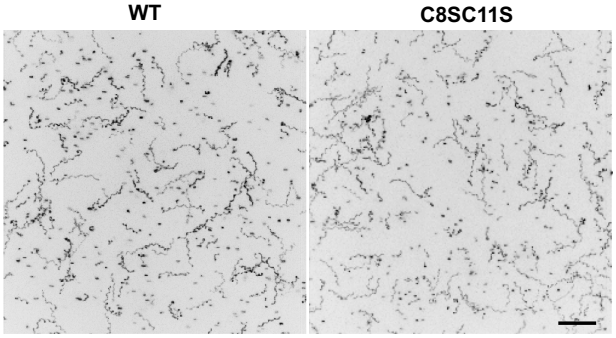

	WT (n = 6)	C8SC11S (n = 6)	*p* value
Total Trajectories Analysed	1859	1433	
% Moving	25.7 ± 4.52	20.2 ± 1.57	0.27
Mean Track Displacement Length (μm)	19.3 ± 0.59	18.2 ± 1.06	0.40
Mean Track Length (μm)	38.9 ± 0.51	34.2 ± 1.80	0.02
Maximum Track Speed (μm/sec)	2.87 ± 0.12	2.56 ± 0.22	0.25
Mean Track Speed (μm/sec)	0.95 ± 0.08	0.83 ± 0.09	0.34

Figure 7

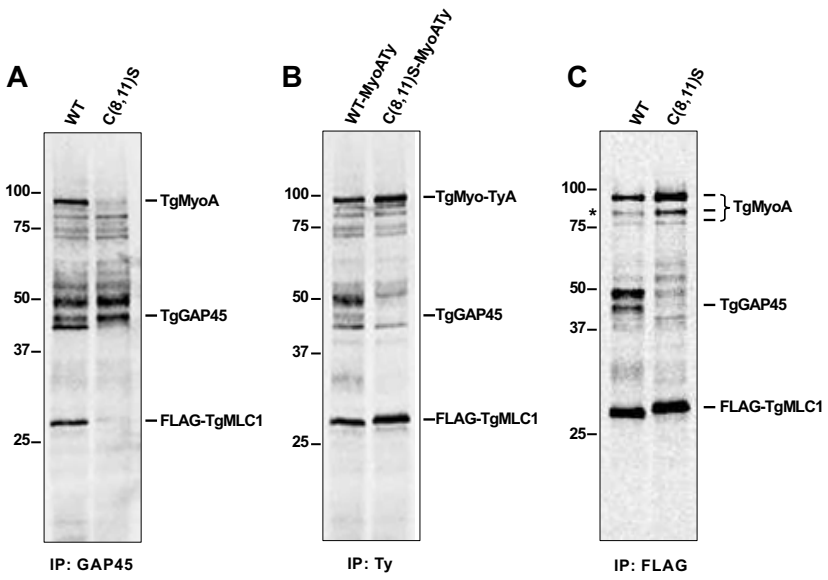

Table 1: Parasite strains used in this study

Strain designation	Relevant genotype
WT	RHΔ*ku80*Δ*mlc1::Flag-MLC1*
C8S	RHΔ*ku80*Δ*mlc1::Flag-MLC1*^{C8S}
C11S	RHΔ*ku80*Δ*mlc1::Flag-MLC1*^{C11S}
C(8,11)S	RHΔ*ku80*Δ*mlc1::Flag-MLC1*^{C8SC11S}
C(8,11)A	RHΔ*ku80*Δ*mlc1::Flag-MLC1*^{C8AC11A}
WT-MyoATy	RHΔ*ku80*Δ*mlc1::Flag-MLC1*Δ*myoA::MYOA-Ty*
C(8,11)S-MyoATy	RHΔ*ku80*Δ*mlc1::Flag-MLC1*^{C8SC11S}Δ*myoA::MYOA-Ty*

Figure S1

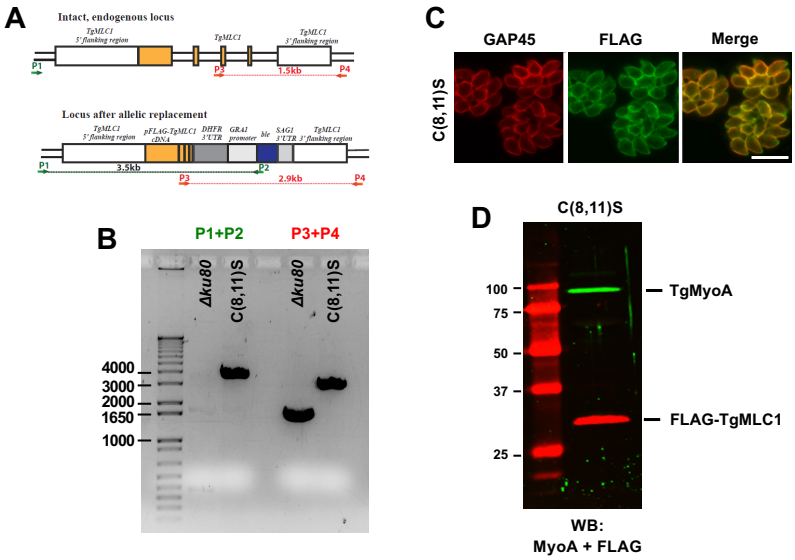

Figure S2

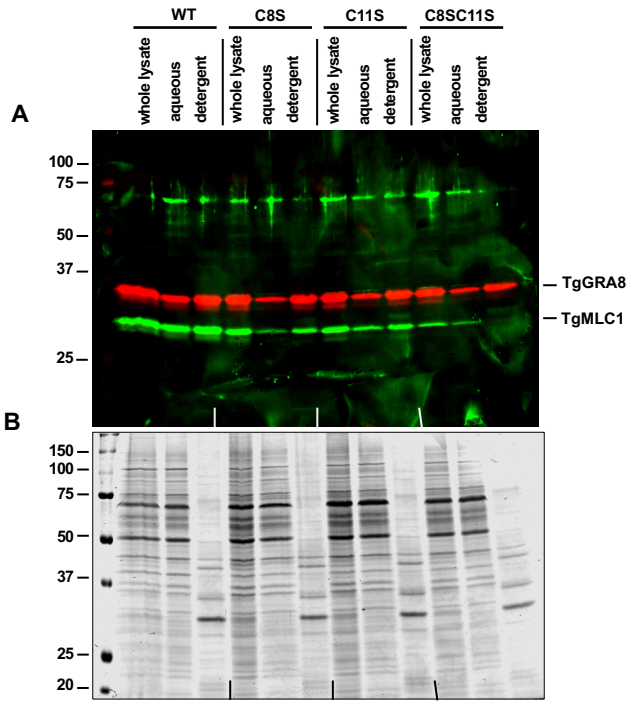

Figure S3

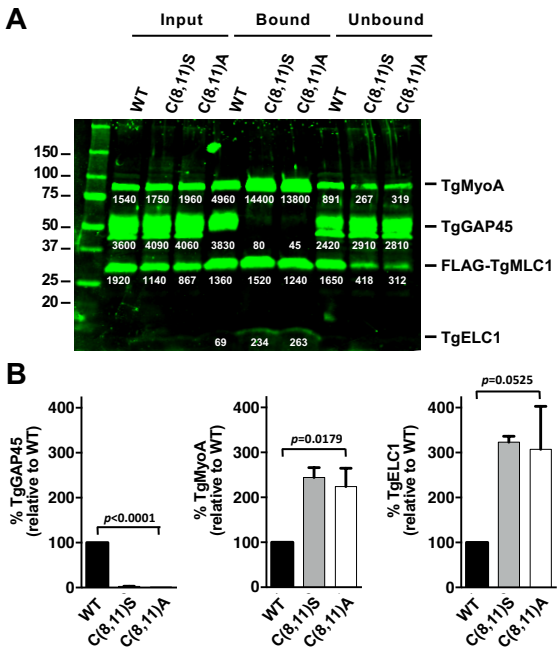

Figure S4

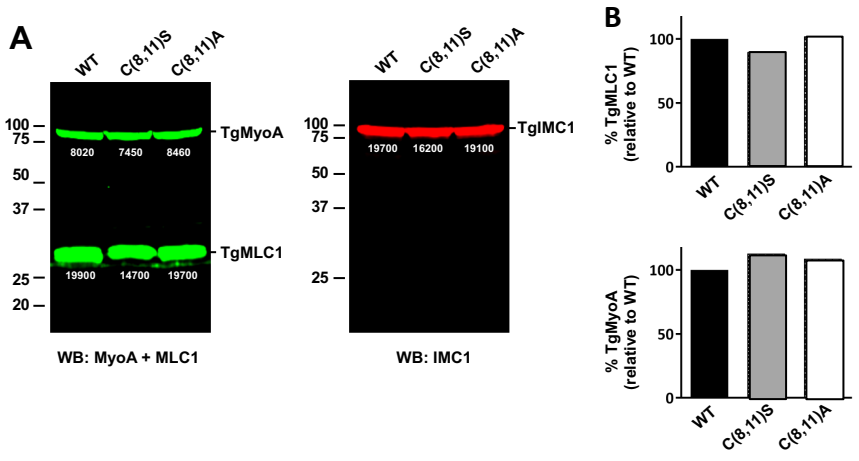

Figure S5

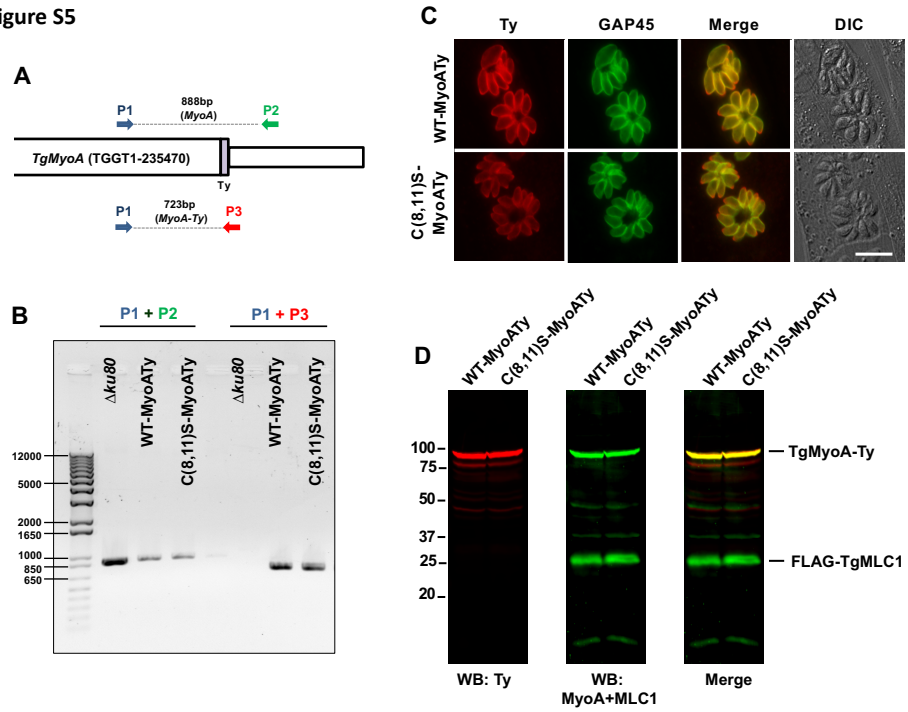

Figure S6

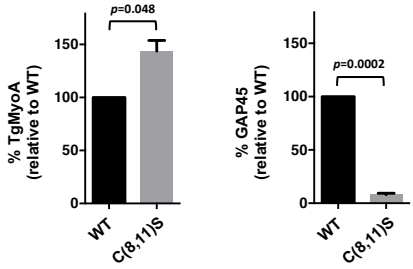

Figure S7

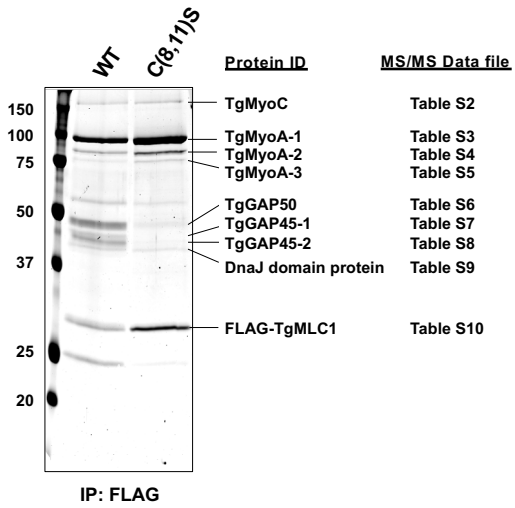

Table S1

Protein name	ToxoDB Accession no.	Score	Sequence Coverage	Unique Peptides	Total spectra (#PSMs)
TgMyoC	TGME49_255190	102.7	23.06	27	36
TgMyoA-1	TGME49_235470	529.7	71.36	63	180
TgMyoA-2	TGME49_235470	231.7	58.97	43	81
TgMyoA-3	TGME49_235470	90.4	32.37	22	32
TgGAP50	TGME49_219320	98.9	34.57	13	28
TgGAP45-1	TGME49_223940	161.2	52.24	15	55
TgGAP45-2	TGME49_223940	255.4	54.69	16	81
DnaJ domain protein	TGME49_267430	47.7	25.41	11	20
TgMLC1	TGME49_257680	124.6	81.22	10	43

TABLE S2

Accession	Description	Score	Coverage	# Proteins	# Unique Peptides	# Peptides	# PSMs	# AAs	MW [kDa]	calc. pI
TGME49_255190	organism=Toxoplasma_gondii_ME49 | product=myosin C | location=TG	102.76	23.06	1	27	27	36	1171	132.6	7.91

A2	Sequence	# PSMs	# Proteins	# Protein Groups	Protein Group Accessions	Modifications	ΔCn	XCorr	Probability	Charge	MH+ [Da]	ΔM [ppm]	RT [min]	# Missed Cleavages
High	RHLEPDSINISPEER	1	1	1	TGME49_255190		0.0000	4.32	0.00	3	1791.89701	-0.82	31.10	1
High	SIIYTTAEPLLVAINPFK	2	1	1	TGME49_255190		0.0000	3.80	0.00	2	1990.12847	1.23	36.58	0
High	HLEPDSINISPEER	2	1	1	TGME49_255190		0.0000	3.77	0.00	3	1635.80051	1.93	31.65	0
High	FmmLDVSSHR	1	1	1	TGME49_255190	M2(Oxidation); M3(Oxidation)	0.0000	3.57	0.00	3	1254.56028	-0.28	30.48	0
High	ADFEEVLQSLDAmQITGSK	1	1	1	TGME49_255190	M13(Oxidation)	0.0000	3.54	0.00	3	2098.00229	0.62	35.54	0
High	TPNFGmAATHIHGSLHVVEQEGmYR	1	1	1	TGME49_255190	M6(Oxidation); M23(Oxidation)	0.0000	3.47	0.00	4	2814.30752	-0.44	32.57	0
High	NFSEFcSHFR	1	1	1	TGME49_255190	C6(Carbamidomethyl)	0.0000	3.22	0.00	3	1330.56379	0.31	32.24	0
High	NQSIIVSGESGAGK	2	1	1	TGME49_255190		0.0000	3.12	0.00	2	1346.69158	0.35	30.26	0
High	KNQSIIVSGESGAGK	1	1	1	TGME49_255190		0.0000	2.95	0.00	3	1474.78580	-0.18	29.83	1
High	RLEPSGFFLESR	1	1	1	TGME49_255190		0.0000	2.94	0.00	3	1437.74851	-0.04	33.30	1
High	STDEGFcGTILR	2	1	1	TGME49_255190	C7(Carbamidomethyl)	0.0000	2.90	0.00	2	1355.62663	0.43	32.47	0
High	FmMLDVSSHR	1	1	1	TGME49_255190	M2(Oxidation)	0.0000	2.84	0.00	3	1238.56610	0.32	31.96	0
High	NASKPEmLPPHVFK	2	1	1	TGME49_255190	M7(Oxidation)	0.0000	2.83	0.00	3	1610.83738	0.85	30.68	0
High	TmVFVKPDAAK	1	1	1	TGME49_255190	M2(Oxidation)	0.0000	2.81	0.00	3	1222.64975	-0.28	30.10	0
High	EALLSGMERPR	1	1	1	TGME49_255190		0.0000	2.78	0.00	3	1258.65772	0.32	31.40	0
High	AALEDLEGYK	2	1	1	TGME49_255190		0.0000	2.75	0.00	2	1108.55266	0.48	32.07	0
High	HFIDVVFDmETK	1	1	1	TGME49_255190	M9(Oxidation)	0.0000	2.74	0.00	3	1496.71259	2.35	33.43	0
High	AALEDLEGYKK	1	1	1	TGME49_255190		0.0000	2.70	0.00	2	1236.64629	-0.66	31.10	1
High	VGPQVIEGVR	1	1	1	TGME49_255190		0.0000	2.66	0.00	2	1053.60564	0.43	30.92	0
High	VVSQEANER	1	1	1	TGME49_255190		0.0000	2.62	0.00	2	1031.51299	1.29	28.35	0
High	TSVLSLSK	2	1	1	TGME49_255190		0.0000	2.62	0.00	1	834.49298	-0.19	31.03	0
High	KSSVVPFGR	1	1	1	TGME49_255190		0.0000	2.46	0.00	2	976.55785	0.37	30.68	1
High	RDFSGIVR	1	1	1	TGME49_255190		0.0000	2.33	0.00	2	949.52196	0.55	30.55	1
High	KEILVK	1	1	1	TGME49_255190		0.0000	2.28	0.00	2	729.48717	0.31	28.99	1
High	SSVVPFGR	2	1	1	TGME49_255190		0.0000	2.27	0.00	2	848.46318	0.78	31.37	0
High	FFASASSEVR	1	1	1	TGME49_255190		0.0000	2.24	0.00	2	1100.53850	1.23	30.92	0
High	QVGYAYR	1	1	1	TGME49_255190		0.0000	2.19	0.00	2	856.43120	0.01	29.75	0
High	KQTQmILGR	1	1	1	TGME49_255190	M5(Oxidation)	0.0000	2.12	0.00	2	1090.60466	0.79	29.32	1

Accession	Description	Score	Coverage	# Proteins	# Unique Peptides	# Peptides	# PSMs	# AAs	MW [kDa]	calc. pI
TGME49_235470	organism=Toxoplasma_gondii_ME49 | product=myosin A | location=TG	66.60	24.55	1	14	14	21	831	93.3	8.16

A2	Sequence	# PSMs	# Proteins	# Protein Groups	Protein Group Accessions	Modifications	ΔCn	XCorr	Probability	Charge	MH+ [Da]	ΔM [ppm]	RT [min]	# Missed Cleavages
High	VSPNINFLISHTVGDIQYNAEGFLFK	1	1	1	TGME49_235470		0.0000	5.05	0.00	3	2923.51297	4.79	36.56	0
High	IFmGmLDIFGFEVFK	1	1	1	TGME49_235470	M3(Oxidation); M5(Oxidation)	0.0000	4.38	0.00	2	1825.89604	3.07	36.56	0
High	NPVVAQLFAGIVMEK	2	1	1	TGME49_235470		0.0000	3.74	0.00	3	1615.88706	-0.41	36.37	0
High	mLIQLHALSVLEALQLR	1	1	1	TGME49_235470	M1(Oxidation)	0.0000	3.65	0.00	3	1964.13718	0.49	36.33	0
High	NNSLEQFFINITNEmLQK	1	1	1	TGME49_235470	M15(Oxidation)	0.0000	3.60	0.00	3	2199.07505	-0.04	36.46	0
High	NQIYTTADPLVVAINPFR	1	1	1	TGME49_235470		0.0000	3.57	0.00	2	2032.09136	2.50	36.02	0
High	NNSVLAALEDQcLAPGGSDEK	1	1	1	TGME49_235470	C12(Carbamidomethyl)	0.0000	3.13	0.00	3	2188.02024	0.67	34.21	0
High	AEImEIVQQSK	3	1	1	TGME49_235470	M4(Oxidation)	0.0000	3.08	0.00	2	1291.65764	1.04	31.05	0
High	YRDTFDLSK	2	1	1	TGME49_235470		0.0000	2.99	0.00	3	1144.56278	-0.50	30.84	1
High	ELIFTSNAEVIK	1	1	1	TGME49_235470		0.0000	2.93	0.00	2	1363.74809	0.93	33.50	0
High	DGGIDDAAAIEGK	2	1	1	TGME49_235470		0.0000	2.88	0.00	2	1231.57915	-0.83	31.09	0
High	LAPHVFYTAR	1	1	1	TGME49_235470		0.0000	2.80	0.00	3	1174.63913	1.99	31.21	0
High	LPSEEYQLGK	1	1	1	TGME49_235470		0.0000	2.72	0.00	2	1163.59453	0.18	30.97	0
High	cIVQAGTDK	2	1	1	TGME49_235470	C1(Carbamidomethyl)	0.0000	2.52	0.00	2	991.48833	0.58	29.35	0
High	AEImEIVQQSK	1	1	1	TGME49_235470		0.0000	2.41	0.00	2	1275.66130	-0.06	32.57	0

Accession	Description	Score	Coverage	# Proteins	# Unique Peptides	# Peptides	# PSMs	# AAs	MW [kDa]	calc. pI
TGME49_233220	organism=Toxoplasma_gondii_ME49 | product=hypothetical protein | loc	12.22	3.73	1	5	5	5	1476	159.6	6.64

A2	Sequence	# PSMs	# Proteins	# Protein Groups	Protein Group Accessions	Modifications	ΔCn	XCorr	Probability	Charge	MH+ [Da]	ΔM [ppm]	RT [min]	# Missed Cleavages
High	KQNSVLETPDVSQTR	1	1	1	TGME49_233220		0.0000	3.12	0.00	3	1701.87815	0.87	30.72	1
High	SGDTPLSVEPPR	1	1	1	TGME49_233220		0.0000	2.41	0.00	2	1254.63469	1.73	31.30	0
High	AAFAVDSSSADK	1	1	1	TGME49_233220		0.0000	2.39	0.00	2	1168.54888	0.65	30.21	0
High	VSSTGNLSK	1	1	1	TGME49_233220		0.0000	2.17	0.00	2	892.47356	0.10	28.50	0
High	LALVLTR	1	1	1	TGME49_233220		0.0000	2.13	0.00	2	785.52452	0.17	32.52	0

Accession	Description	Score	Coverage	# Proteins	# Unique Peptides	# Peptides	# PSMs	# AAs	MW [kDa]	calc. pI
TGME49_257680	organism=Toxoplasma_gondii_ME49 | product=myosin light chain MLC1	4.60	10.80	1	2	2	2	213	24.1	4.65

A2	Sequence	# PSMs	# Proteins	# Protein Groups	Protein Group Accessions	Modifications	ΔCn	XCorr	Probability	Charge	MH+ [Da]	ΔM [ppm]	RT [min]	# Missed Cleavages
High	VSTGDAmILAR	1	1	1	TGME49_257680	M7(Oxidation)	0.0000	2.45	0.00	2	1149.59453	1.06	30.85	0
High	SGDNLDYASFQK	1	1	1	TGME49_257680		0.0000	2.15	0.00	2	1344.60735	0.50	31.58	0

TABLE S3

Accession	Description	Score	Coverage	# Proteins	# Unique Peptides	# Peptides	# PSMs	# AAs	MW [kDa]	calc. pI
TGME49_235470	organism=Toxoplasma_gondii_ME49 | product=myosin A | location=TG	529.76	71.36	1	63	64	180	831	93.3	8.16

A2	Sequence	# PSMs	# Proteins	# Protein Groups	Protein Group Accessions	Modifications	ΔCn	XCorr	Probability	Charge	MH+ [Da]	ΔM [ppm]	RT [min]	# Missed Cleavages
High	VSPNINFLISHTVGDIQYNAEGFLFK	3	1	1	TGME49_235470		0.0000	6.79	0.00	2	2923.50420	1.78	36.58	0
High	SSDVHAVDHSGNVYK	5	1	1	TGME49_235470		0.0000	6.07	0.00	3	1614.75199	0.78	29.13	0
High	RSSDVHAVDHSGNVYK	2	1	1	TGME49_235470		0.0000	5.80	0.00	4	1770.85207	0.13	29.02	1
High	ALDNLHAVNKSQTIIVSGESGAGK	2	1	1	TGME49_235470		0.0000	5.38	0.00	3	2409.27610	1.14	31.52	1
High	EcLSSWEPLVSVLEAYYAGR	1	1	1	TGME49_235470	C2(Carbamidomethyl)	0.0000	5.37	0.00	2	2329.11992	1.26	36.62	0
High	SQTIIVSGESGAGKTEATK	2	1	1	TGME49_235470		0.0000	5.01	0.00	3	1863.96750	0.86	29.98	1
High	NNSVLAALEDQcLAPGGSDEK	5	1	1	TGME49_235470	C12(Carbamidomethyl)	0.0000	4.68	0.00	3	2188.02665	3.60	34.07	0
High	KRSsDVHAVDHSGNVYK	2	1	1	TGME49_235470	S4(Phospho)	0.0000	4.65	0.00	3	1978.91489	0.88	28.97	2
High	NQIYTTADPLVVAINPFR	2	1	1	TGME49_235470		0.0000	4.53	0.00	2	2032.09001	1.84	35.87	0
High	GQLIGSQFLSQLQSLmELINSTEPHFIR	2	1	1	TGME49_235470	M16(Oxidation)	0.0000	4.52	0.00	4	3202.67129	4.57	36.65	0
High	NNSLEQFFINITTNEmLQK	3	1	1	TGME49_235470	M15(Oxidation)	0.0000	4.49	0.00	2	2199.07915	1.82	36.43	0
High	IFmGmLDIFGFEVFK	2	1	1	TGME49_235470	M3(Oxidation); M5(Oxidation)	0.0000	4.47	0.00	2	1825.89592	3.00	36.58	0
High	GFQIWTDLAPSVKEEPDLmFAK	1	1	1	TGME49_235470	M19(Oxidation)	0.0000	4.42	0.00	3	2538.26108	0.97	35.29	1
High	ELIFTSNAEVIKILTAK	1	1	1	TGME49_235470		0.0000	4.38	0.00	3	1890.09323	-0.79	35.57	1
High	IQNAIMAANPVLEAFGNAK	1	1	1	TGME49_235470		0.0000	4.34	0.00	3	1972.03415	1.00	35.64	0
High	DEGVSSKELIFTSNAEVIK	1	1	1	TGME49_235470		0.0000	4.25	0.00	3	2066.06357	-0.83	33.32	1
High	KAcGLLFLDAER	4	1	1	TGME49_235470	C3(Carbamidomethyl)	0.0000	4.24	0.00	2	1392.73088	0.29	33.41	1
High	IFMGmLDIFGFEVFK	2	1	1	TGME49_235470	M5(Oxidation)	0.0000	3.99	0.00	2	1809.89617	0.35	36.63	0
High	mLIQLHALSVLEALQLR	2	1	1	TGME49_235470	M1(Oxidation)	0.0000	3.86	0.00	2	1964.13542	-0.41	36.21	0
High	NPVVAQLFAGIVMEK	2	1	1	TGME49_235470		0.0000	3.83	0.00	2	1615.89446	4.17	36.21	0
High	NPVVAQLFAGIVmEK	2	1	1	TGME49_235470	M13(Oxidation)	0.0000	3.77	0.00	2	1631.88457	1.18	45.73	0
High	DGGIDDAAAIEGK	8	1	1	TGME49_235470		0.0000	3.77	0.00	2	1231.58122	0.86	30.85	0
High	GQLIGSQFLSQLQSLMELINSTEPHFIR	1	1	1	TGME49_235470		0.0000	3.75	0.00	4	3186.66836	2.08	36.73	0
High	SQTIIVSGESGAGK	8	1	1	TGME49_235470		0.0000	3.67	0.00	2	1333.69390	-1.47	31.25	0
High	DGGIDDAAAIEGKNLEVFK	1	1	1	TGME49_235470		0.0000	3.61	0.00	3	1961.98185	0.13	33.58	1
High	NPVVAQLFAGIVmEKGK	1	1	1	TGME49_235470	M13(Oxidation)	0.0000	3.56	0.00	3	1817.00022	0.63	35.16	1
High	QTGAKELTQIQR	2	1	1	TGME49_235470		0.0000	3.53	0.00	3	1372.75531	0.69	29.96	1
High	SYHIFYQMcK	3	1	1	TGME49_235470	C9(Carbamidomethyl)	0.0000	3.45	0.00	2	1376.61260	-0.01	32.34	0
High	YINPLcLDAPGIDDVAEFHEVcESFR	1	1	1	TGME49_235470	C6(Carbamidomethyl); C22(Carbamidomethyl)	0.0000	3.43	0.00	3	3066.40555	2.68	35.37	0
High	YRDTFDLSK	2	1	1	TGME49_235470		0.0000	3.40	0.00	2	1144.56316	-0.17	30.69	1
High	IQNAImAANPVLEAFGNAKTIR	1	1	1	TGME49_235470	M6(Oxidation)	0.0000	3.37	0.00	3	2358.25925	-0.30	34.66	1
High	LFmWIIAVLNR	2	1	1	TGME49_235470	M3(Oxidation)	0.0000	3.35	0.00	2	1391.78826	1.00	36.60	0
High	TTSEELKTATALK	2	1	1	TGME49_235470		0.0000	3.31	0.00	3	1392.75812	0.01	30.52	1
High	ALDNLHAVNK	2	1	1	TGME49_235470		0.0000	3.31	0.00	2	1094.59538	0.05	29.67	0
High	TmVFLKQTGAK	1	1	1	TGME49_235470	M2(Oxidation)	0.0000	3.29	0.00	3	1239.67902	1.92	29.98	1
High	SSKLPSEEYQLGK	1	1	1	TGME49_235470		0.0000	3.28	0.00	3	1465.75385	0.34	30.71	1
High	AEImEIVQQSK	5	1	1	TGME49_235470	M4(Oxidation)	0.0000	3.26	0.00	2	1291.65373	-1.98	30.83	0
High	ELIFTSNAEVIK	4	1	1	TGME49_235470		0.0000	3.26	0.00	2	1363.74797	0.84	33.55	0
High	FGSVVAFLLEK	2	1	1	TGME49_235470		0.0000	3.22	0.00	2	1209.68779	-0.05	35.93	0
High	RALDNLHAVNK	2	1	1	TGME49_235470		0.0000	3.21	0.00	3	1250.69611	-0.27	29.62	1
High	GFQIWTDLAPSVK	4	1	1	TGME49_235470		0.0000	3.08	0.00	2	1461.77312	-0.41	35.19	0
High	FHILPLSEYK	2	1	1	TGME49_235470		0.0000	3.08	0.00	2	1246.68315	0.07	33.33	0
High	AcGLLFLDAER	1	1	1	TGME49_235470	C2(Carbamidomethyl)	0.0000	3.03	0.00	2	1264.63664	0.90	34.46	0
High	KPLDWVPSK	3	1	1	TGME49_235470		0.0000	3.02	0.00	2	1069.60564	1.43	31.41	0
High	RPFKEFLFQFK	1	1	1	TGME49_235470		0.0000	2.96	0.00	3	1486.82352	1.96	33.91	1
High	cIVQAGTDK	8	1	1	TGME49_235470	C1(Carbamidomethyl)	0.0000	2.93	0.00	2	991.48741	-0.34	29.34	0
High	AEIMEIVQQSK	2	1	1	TGME49_235470		0.0000	2.92	0.00	3	1275.66291	1.20	32.59	0
High	DLGNTTLDWIVR	4	1	1	TGME49_235470		0.0000	2.78	0.00	2	1402.73296	0.28	35.57	0
High	RSsDVHAVDHSGNVYK	8	1	1	TGME49_235470	S3(Phospho)	0.0000	2.73	0.00	2	1850.81938	0.65	29.15	1
High	LPSEEYQLGKTmVFLK	1	1	1	TGME49_235470	M12(Oxidation)	0.0000	2.66	0.00	3	1898.99430	0.53	33.24	1
High	VSYAGNQEIR	3	1	1	TGME49_235470		0.0000	2.66	0.00	2	1136.57097	1.29	29.86	0
High	FLSTcKNALK	1	1	1	TGME49_235470	C5(Carbamidomethyl)	0.0000	2.65	0.00	3	1181.63486	0.09	30.00	1
High	TATALK	9	1	1	TGME49_235470		0.0000	2.64	0.00	1	604.36639	-0.14	22.95	0
High	NPVDIVFDR	8	1	1	TGME49_235470		0.0000	2.62	0.00	2	1124.57549	1.73	34.99	0
High	VLTQDEQER	7	1	1	TGME49_235470		0.0000	2.61	0.00	2	1117.54985	1.26	45.69	0
High	FGSVVAFLLEKSR	1	1	1	TGME49_235470		0.0000	2.51	0.00	3	1452.82276	1.21	35.26	1
High	LAPHVFYTAR	1	1	1	TGME49_235470		0.0000	2.48	0.00	3	1174.63666	-0.11	30.99	0
High	FmKNQIYTTADPLVVAINPFR	1	1	1	TGME49_235470	M2(Oxidation)	0.0000	2.46	0.00	3	2454.28141	-1.50	35.49	1
High	cIKPNDTK	1	1	1	TGME49_235470	C1(Carbamidomethyl)	0.0000	2.44	0.00	2	975.49352	0.70	27.85	0
High	GADAAMK	1	1	1	TGME49_235470		0.0000	2.43	0.00	1	663.31256	-0.80	18.57	0
High	TmVFLK	1	1	1	TGME49_235470	M2(Oxidation)	0.0000	2.39	0.00	2	754.41667	-0.19	30.57	0
High	TGSMDLR	1	1	1	TGME49_235470		0.0000	2.38	0.00	2	779.37230	0.82	29.38	0
High	SsDVHAVDHSGNVYK	4	1	1	TGME49_235470	S2(Phospho)	0.0000	2.36	0.00	3	1694.71653	-0.31	29.35	0
High	TEATKQIMR	1	2	2	TGME49_235470 ;TGME49_255190		0.0000	2.29	0.00	2	1077.57219	0.03	29.10	1
High	LPSEEYQLGK	1	1	1	TGME49_235470		0.0000	2.28	0.00	2	1163.59551	1.02	30.94	0
High	QLGYSYR	1	1	1	TGME49_235470		0.0000	2.28	0.00	2	886.44206	0.35	30.05	0
High	SYHIFYQmcK	2	1	1	TGME49_235470	M8(Oxidation); C9(Carbamidomethyl)	0.0000	2.25	0.00	2	1392.60759	0.04	30.99	0
High	DEGVSSK	1	1	1	TGME49_235470		0.0000	2.21	0.00	1	721.33398	-3.23	15.76	0
High	FMQLDVGR	1	1	1	TGME49_235470		0.0000	2.20	0.00	2	965.48821	0.87	32.24	0
High	TTSEELK	2	1	1	TGME49_235470		0.0000	2.18	0.00	2	807.40862	-1.06	28.02	0
High	TATALKK	1	1	1	TGME49_235470		0.0000	2.18	0.00	2	732.46141	-0.05	20.60	1
High	TMVFLK	1	1	1	TGME49_235470		0.0000	2.18	0.00	2	738.42241	0.69	32.13	0

Accession	Description	Score	Coverage	# Proteins	# Unique Peptides	# Peptides	# PSMs	# AAs	MW [kDa]	calc. pI
TGME49_233220	organism=Toxoplasma_gondii_ME49 | product=hypothetical protein | loc	6.38	2.51	1	2	2	2	1476	159.6	6.64

A2	Sequence	# PSMs	# Proteins	# Protein Groups	Protein Group Accessions	Modifications	ΔCn	XCorr	Probability	Charge	MH+ [Da]	ΔM [ppm]	RT [min]	# Missed Cleavages
High	SATVNQGEGQPTEFAIDATDDGHK	1	1	1	TGME49_233220		0.0000	3.92	0.00	3	2488.11875	-1.46	31.74	0
High	TVNSmEEFASLVR	1	1	1	TGME49_233220	M5(Oxidation)	0.0000	2.46	0.00	2	1498.72075	0.04	33.11	0

Accession	Description	Score	Coverage	# Proteins	# Unique Peptides	# Peptides	# PSMs	# AAs	MW [kDa]	calc. pI
TGME49_255190	organism=Toxoplasma_gondii_ME49 | product=myosin C | location=TG	4.67	1.62	1	1	2	2	1171	132.6	7.91

A2	Sequence	# PSMs	# Proteins	# Protein Groups	Protein Group Accessions	Modifications	ΔCn	XCorr	Probability	Charge	MH+ [Da]	ΔM [ppm]	RT [min]	# Missed Cleavages
High	VGPQVIEGVR	1	1	1	TGME49_255190		0.0000	2.38	0.00	2	1053.60613	0.90	31.29	0
High	TEATKQIMR	1	2	2	TGME49_235470 ;TGME49_255190		0.0000	2.29	0.00	2	1077.57219	0.03	29.10	1

TABLE S4

Accession	Description	Score	Coverage	# Proteins	# Unique Peptides	# Peptides	# PSMs	# AAs	MW [kDa]	calc. pI
TGME49_235470	organism=Toxoplasma_gondii_ME49 | product=myosin A | location=TG	231.70	58.97	2	43	44	81	831	93.3	8.16

A2	Sequence	# PSMs	# Proteins	# Protein Groups	Protein Group Accessions	Modifications	ΔCn	XCorr	Probability	Charge	MH+ [Da]	ΔM [ppm]	RT [min]	# Missed Cleavages
High	EcLSSWEPLVSVLEAYYAGR	1	1	1	TGME49_235470	C2(Carbamidomethyl)	0.0000	5.32	0.00	2	2329.12163	1.99	36.69	0
High	YINPLcLDAPGIDDVAEFHEVcESFR	1	1	1	TGME49_235470	C6(Carbamidomethyl); C22(Carbami	0.0000	4.78	0.00	4	3066.39589	-0.46	35.77	0
High	mLIQLHALSVLEALQLR	3	1	1	TGME49_235470	M1(Oxidation)	0.0000	4.60	0.00	3	1964.13736	0.58	36.39	0
High	SQTIIVSGESGAGKTEATK	1	1	1	TGME49_235470		0.0000	4.57	0.00	3	1863.96714	0.66	30.15	1
High	NNSLEQFFINITNEmLQK	2	1	1	TGME49_235470	M15(Oxidation)	0.0000	4.43	0.00	2	2199.07939	1.94	36.54	0
High	IFmGmLDIFGFEVFK	1	1	1	TGME49_235470	M3(Oxidation); M5(Oxidation)	0.0000	4.10	0.00	2	1825.89226	1.00	36.64	0
High	NPVVAQLFAGIVMEK	2	1	1	TGME49_235470		0.0000	4.08	0.00	2	1615.88811	0.24	36.41	0
High	NQIYTTADPLVVAINPFR	1	1	1	TGME49_235470		0.0000	4.05	0.00	3	2032.08908	1.38	36.04	0
High	NNSVLAALEDQcLAPGGSDEK	3	1	1	TGME49_235470	C12(Carbamidomethyl)	0.0000	3.92	0.00	3	2188.02134	1.17	34.22	0
High	GQLIGSQFLSQLQSLmELINSTEPHFIR	1	1	1	TGME49_235470	M16(Oxidation)	0.0000	3.75	0.00	3	3202.67063	4.37	36.72	0
High	SQTIIVSGESGAGK	4	1	1	TGME49_235470		0.0000	3.51	0.00	2	1333.69634	0.36	30.44	0
High	IQNAIMAANPVLEAFGNAK	1	1	1	TGME49_235470		0.0000	3.49	0.00	3	1972.03305	0.45	35.79	0
High	KAcGLLFLDAER	2	1	1	TGME49_235470	C3(Carbamidomethyl)	0.0000	3.44	0.00	2	1392.73296	1.78	33.72	1
High	LYRDEGVSSK	1	1	1	TGME49_235470		0.0000	3.44	0.00	2	1153.58440	-0.37	28.92	1
High	ELIFTSNAEVIK	2	1	1	TGME49_235470		0.0000	3.41	0.00	2	1363.74748	0.49	33.57	0
High	AEImEIVQQSK	2	1	1	TGME49_235470	M4(Oxidation)	0.0000	3.34	0.00	2	1291.65679	0.38	31.07	0
High	DGGIDDAAAIEGK	3	1	1	TGME49_235470		0.0000	3.26	0.00	2	1231.58147	1.05	31.28	0
High	ALDNLHAVNK	2	1	1	TGME49_235470		0.0000	3.22	0.00	3	1094.59375	-1.44	29.86	0
High	FGSVVAFLLEK	1	1	1	TGME49_235470		0.0000	3.10	0.00	2	1209.68840	0.46	36.05	0
High	LFmWIIAVLNR	1	1	1	TGME49_235470	M3(Oxidation)	0.0000	3.10	0.00	2	1391.78716	0.21	36.69	0
High	DEGVSSKELIFTSNAEVIK	1	1	1	TGME49_235470		0.0000	3.06	0.00	3	2066.05716	-3.93	33.48	1
High	IFMGmLDIFGFEVFK	2	1	1	TGME49_235470	M5(Oxidation)	0.0000	3.04	0.00	2	1809.89861	1.70	36.71	0
High	ELIFTSNAEVIKILTAK	1	1	1	TGME49_235470		0.0000	3.02	0.00	3	1890.09922	2.37	35.72	1
High	AEIMEIVQQSK	2	1	1	TGME49_235470		0.0000	3.00	0.00	2	1275.66130	-0.06	32.73	0
High	RALDNLHAVNK	2	1	1	TGME49_235470		0.0000	2.95	0.00	3	1250.69602	-0.35	29.68	1
High	SYHIFYQMcK	2	1	1	TGME49_235470	C9(Carbamidomethyl)	0.0000	2.95	0.00	3	1376.61426	1.20	32.49	0
High	FHILPLSEYK	2	1	1	TGME49_235470		0.0000	2.89	0.00	2	1246.68376	0.56	33.59	0
High	NFVDIVFDR	4	1	1	TGME49_235470		0.0000	2.89	0.00	2	1124.57402	0.43	35.15	0
High	RPFKEFLFQFK	1	1	1	TGME49_235470		0.0000	2.75	0.00	3	1486.82224	1.10	34.11	1
High	KPLDWVPSK	1	1	1	TGME49_235470		0.0000	2.74	0.00	2	1069.60222	-1.77	31.57	0
High	YRDTFDLSK	2	1	1	TGME49_235470		0.0000	2.73	0.00	2	1144.56365	0.26	30.93	1
High	ALDNLHAVNKSQTIIVSGESGAGK	1	1	1	TGME49_235470		0.0000	2.64	0.00	3	2409.27793	1.90	31.86	1
High	cIKPNDTK	2	1	1	TGME49_235470	C1(Carbamidomethyl)	0.0000	2.61	0.00	2	975.49315	0.32	27.58	0
High	SYHIFYQmcK	1	1	1	TGME49_235470	M8(Oxidation); C9(Carbamidomethyl	0.0000	2.59	0.00	3	1392.60999	1.77	31.31	0
High	NPVVAQLFAGIVmEKGK	1	1	1	TGME49_235470	M13(Oxidation)	0.0000	2.55	0.00	3	1817.00187	1.53	35.38	1
High	NPVVAQLFAGIVmEK	1	1	1	TGME49_235470	M13(Oxidation)	0.0000	2.49	0.00	2	1631.88188	-0.46	35.90	0
High	VLTQDEQER	4	1	1	TGME49_235470		0.0000	2.46	0.00	2	1117.54973	1.15	28.98	0
High	DLGNTTLDWIVR	2	1	1	TGME49_235470		0.0000	2.44	0.00	2	1402.73345	0.62	35.41	0
High	VSPNINFLISHTVGDIQYNAEGFLFK	1	1	1	TGME49_235470		0.0000	2.41	0.00	3	2923.50602	2.41	36.52	0
High	LPSEEYQLGK	1	1	1	TGME49_235470		0.0000	2.38	0.00	2	1163.59551	1.02	31.20	0
High	TEATKQImR	1	2	2	TGME49_235470 ;TGME49_255190	M8(Oxidation)	0.0000	2.35	0.00	3	1093.56699	-0.08	28.52	1
High	RSSDVHAVDHSGNVYK	1	1	1	TGME49_235470		0.0000	2.33	0.00	4	1770.85293	0.61	29.20	1
High	TmVFLK	1	1	1	TGME49_235470	M2(Oxidation)	0.0000	2.24	0.00	2	754.41637	-0.59	30.88	0
High	TGSMDLR	2	1	1	TGME49_235470		0.0000	2.22	0.00	2	779.37151	-0.20	29.68	0
High	LAPHVFYTAR	3	1	1	TGME49_235470		0.0000	2.19	0.00	3	1174.63703	0.20	31.46	0
High	SRVLTQDEQER	1	1	1	TGME49_235470		0.0000	2.16	0.00	3	1360.68354	1.43	29.05	1
High	TMVFLK	1	1	1	TGME49_235470		0.0000	2.16	0.00	2	738.42235	0.61	32.44	0
High	QEDGDmLK	1	1	1	TGME49_235470	M6(Oxidation)	0.0000	2.15	0.00	2	951.40959	0.79	28.25	0
High	ILTAK	1	2	1	TGME49_235470		0.0000	1.79	0.00	1	545.36597	0.40	28.40	0
TGME49_233220	organism=Toxoplasma_gondii_ME49 | product=hypothetical protein | loc	15.07	5.49	1	6	6	6	1476	159.6	6.64

A2	Sequence	# PSMs	# Proteins	# Protein Groups	Protein Group Accessions	Modifications	ΔCn	XCorr	Probability	Charge	MH+ [Da]	ΔM [ppm]	RT [min]	# Missed Cleavages
High	TQLGSLSSSVSTLAPGASVR	1	1	1	TGME49_233220		0.0000	2.81	0.00	2	1918.02580	0.90	33.50	0
High	AAFAVDSSSADK	1	1	1	TGME49_233220		0.0000	2.63	0.00	2	1168.54875	0.54	30.20	0
High	TAAPIHTQNQAVR	1	1	1	TGME49_233220		0.0000	2.62	0.00	3	1406.74967	-0.19	29.43	0
High	KQNSVLETPDVSQTR	1	1	1	TGME49_233220		0.0000	2.50	0.00	3	1701.87943	1.62	30.81	1
High	VSTVSPTTSVSGDR	1	1	1	TGME49_233220		0.0000	2.37	0.00	2	1392.69573	-0.61	30.01	0
High	LALVLTR	1	1	1	TGME49_233220		0.0000	2.13	0.00	2	785.52458	0.24	32.71	0
TGME49_219850	organism=Toxoplasma_gondii_ME49 | product=prolyl-tRNA synthetase (	13.62	8.80	1	5	5	5	830	93.4	8.07

A2	Sequence	# PSMs	# Proteins	# Protein Groups	Protein Group Accessions	Modifications	ΔCn	XCorr	Probability	Charge	MH+ [Da]	ΔM [ppm]	RT [min]	# Missed Cleavages
High	LAAAPAGGANKPNAPAGK	1	1	1	TGME49_219850		0.0000	3.10	0.00	3	1575.86094	0.42	29.41	0
High	EAVTDSSmLGVTAK	1	1	1	TGME49_219850	M8(Oxidation)	0.0000	2.75	0.00	2	1424.69292	-0.63	30.59	0
High	LEELGIGYQLHR	1	1	1	TGME49_219850		0.0000	2.71	0.00	3	1427.76468	0.34	32.88	0
High	ISTFDEVmPALNR	1	1	1	TGME49_219850	M8(Oxidation)	0.0000	2.60	0.00	2	1508.74199	0.37	32.70	0
High	GIQAATSHLLGTNFAK	1	1	1	TGME49_219850		0.0000	2.46	0.00	3	1628.87894	2.08	33.17	0
TGME49_255190	organism=Toxoplasma_gondii_ME49 | product=myosin C | location=TG	6.64	2.65	1	2	3	3	1171	132.6	7.91

A2	Sequence	# PSMs	# Proteins	# Protein Groups	Protein Group Accessions	Modifications	ΔCn	XCorr	Probability	Charge	MH+ [Da]	ΔM [ppm]	RT [min]	# Missed Cleavages
High	TEATKQImR	1	2	2	TGME49_235470 ;TGME49_255190	M8(Oxidation)	0.0000	2.35	0.00	3	1093.56699	-0.08	28.52	1
High	RLEPSGFFLESR	1	1	1	TGME49_255190		0.0000	2.17	0.00	3	1437.74649	-1.44	33.48	1
High	VGPQVIEGVR	1	1	1	TGME49_255190		0.0000	2.11	0.00	2	1053.60759	2.29	31.52	0
TGME49_266640	organism=Toxoplasma_gondii_ME49 | product=Acetyl-coenzyme A synth	5.32	3.22	1	2	2	2	714	79.9	6.89

A2	Sequence	# PSMs	# Proteins	# Protein Groups	Protein Group Accessions	Modifications	ΔCn	XCorr	Probability	Charge	MH+ [Da]	ΔM [ppm]	RT [min]	# Missed Cleavages
High	VDDTLNVSGHR	1	1	1	TGME49_266640		0.0000	2.84	0.00	3	1212.59607	-0.59	29.92	0
High	ASQFYTAPTALR	1	1	1	TGME49_266640		0.0000	2.47	0.00	2	1325.68511	0.18	32.40	0
TGME49_249850	organism=Toxoplasma_gondii_ME49 | product=GAP40 protein (GAP40) |	2.39	2.08	1	1	1	1	385	43.1	6.62

A2	Sequence	# PSMs	# Proteins	# Protein Groups	Protein Group Accessions	Modifications	ΔCn	XCorr	Probability	Charge	MH+ [Da]	ΔM [ppm]	RT [min]	# Missed Cleavages
High	LPTWQQIR	1	1	1	TGME49_249850		0.0000	2.39	0.00	2	1041.58440	0.35	32.84	0
TGME49_219320	organism=Toxoplasma_gondii_ME49 | product=acid phosphatase GAP50	2.19	2.55	1	1	1	1	431	46.6	6.95

A2	Sequence	# PSMs	# Proteins	# Protein Groups	Protein Group Accessions	Modifications	ΔCn	XCorr	Probability	Charge	MH+ [Da]	ΔM [ppm]	RT [min]	# Missed Cleavages
High	ILDYIIVVADR	1	1	1	TGME49_219320		0.0000	2.19	0.00	2	1289.74626	-0.12	35.05	0
TGME49_235402	organism=Toxoplasma_gondii_ME49 | product=CorA family Mg2+ transp	2.17	0.76	1	1	1	1	1187	127.5	8.62

A2	Sequence	# PSMs	# Proteins	# Protein Groups	Protein Group Accessions	Modifications	ΔCn	XCorr	Probability	Charge	MH+ [Da]	ΔM [ppm]	RT [min]	# Missed Cleavages
High	GVATVSLPR	1	1	1	TGME49_235402		0.0000	2.17	0.00	2	899.53105	0.12	31.21	0

TABLE S5

Accession	Description	Score	Coverage	# Proteins	# Unique Peptides	# Peptides	# PSMs	# AAs	MW [kDa]	calc. pI
TGME49_235470	organism=Toxoplasma_gondii_ME49 | product=myosin A | location=TG	90.48	32.37	1	22	22	32	831	93.3	8.16

	A2	Sequence	# PSMs	# Proteins	# Protein Groups	Protein Group Accessions	Modifications	ΔCn	XCorr	Probability	Charge	MH+ [Da]	ΔM [ppm]	RT [min]	# Missed Cleavages
	High	mLIQLHALSVLEALQLR	2	1	1	TGME49_235470	M1(Oxidation)	0.0000	4.09	0.00	3	1964.13810	0.95	36.60	0
	High	NNSLEQFFINITNEmLQK	1	1	1	TGME49_235470	M15(Oxidation)	0.0000	3.95	0.00	3	2199.07541	0.13	36.69	0
	High	IFmGmLDIFGFEVFK	1	1	1	TGME49_235470	M3(Oxidation); M5(Oxidation)	0.0000	3.90	0.00	2	1825.89238	1.06	36.79	0
	High	NNSLEQFFINITNEMLQK	1	1	1	TGME49_235470		0.0000	3.89	0.00	3	2183.08261	1.10	36.88	0
	High	NNSVLAALEDQcLAPGGSDEK	3	1	1	TGME49_235470	C12(Carbamidomethyl)	0.0000	3.82	0.00	3	2188.02005	0.59	34.44	0
	High	DGGIDDAAAIEGK	3	1	1	TGME49_235470		0.0000	3.35	0.00	2	1231.58049	0.26	31.32	0
	High	NPVVAQLFAGIVMEK	2	1	1	TGME49_235470		0.0000	3.26	0.00	2	1615.88994	1.37	36.60	0
	High	YRDTFDLSK	2	1	1	TGME49_235470		0.0000	3.21	0.00	3	1144.56324	-0.10	31.10	1
	High	RALDNLHAVNK	1	1	1	TGME49_235470		0.0000	3.21	0.00	3	1250.69675	0.24	29.92	1
	High	ELIFTSNAEVIK	1	1	1	TGME49_235470		0.0000	3.13	0.00	2	1363.74687	0.04	33.77	0
	High	AEImElVQQSK	1	1	1	TGME49_235470	M4(Oxidation)	0.0000	2.96	0.00	2	1291.65715	0.66	31.20	0
	High	LYRDEGVSSK	1	1	1	TGME49_235470		0.0000	2.94	0.00	3	1153.58466	-0.14	29.09	1
	High	LPSEEYQLGK	1	1	1	TGME49_235470		0.0000	2.78	0.00	2	1163.59429	-0.03	31.20	0
	High	FHILPLSEYK	2	1	1	TGME49_235470		0.0000	2.67	0.00	3	1246.68372	0.52	33.82	0
	High	IQNAImAANPVLEAFGNAK	1	1	1	TGME49_235470	M6(Oxidation)	0.0000	2.66	0.00	3	1988.02823	0.58	35.10	0
	High	LAPHVFYTAR	2	1	1	TGME49_235470		0.0000	2.66	0.00	3	1174.63749	0.59	31.47	0
	High	DLGNTTLDWIVR	1	1	1	TGME49_235470		0.0000	2.66	0.00	2	1402.73320	0.45	35.41	0
	High	SQTIIVSGESGAGK	1	1	1	TGME49_235470		0.0000	2.54	0.00	2	1333.69634	0.36	30.63	0
	High	cIVQAGTDK	1	1	1	TGME49_235470	C1(Carbamidomethyl)	0.0000	2.45	0.00	2	991.48747	-0.28	29.58	0
	High	VSYAGNQEIR	1	1	1	TGME49_235470		0.0000	2.15	0.00	2	1136.57048	0.86	30.20	0
	High	KAcGLLFLDAER	1	1	1	TGME49_235470	C3(Carbamidomethyl)	0.0000	2.09	0.00	2	1392.72991	-0.41	33.97	1
	High	FLSTcK	1	1	1	TGME49_235470	C5(Carbamidomethyl)	0.0000	1.56	0.00	1	755.37537	-0.40	29.52	0
	High	ILTAK	1	1	1	TGME49_235470		0.0000	1.41	0.00	1	545.36621	0.84	28.06	0

TGME49_233220	organism=Toxoplasma_gondii_ME49 | product=hypothetical protein | loc	42.44	9.82	1	13	13	16	1476	159.6	6.64

	A2	Sequence	# PSMs	# Proteins	# Protein Groups	Protein Group Accessions	Modifications	ΔCn	XCorr	Probability	Charge	MH+ [Da]	ΔM [ppm]	RT [min]	# Missed Cleavages
	High	TQLGSLSSSVSTLAPGASVR	1	1	1	TGME49_233220		0.0000	4.12	0.00	3	1918.02555	0.76	33.66	0
	High	KTAAPIHTQNQAVR	2	1	1	TGME49_233220		0.0000	3.59	0.00	3	1534.84476	-0.10	29.17	1
	High	TAAPIHTQNQAVR	1	1	1	TGME49_233220		0.0000	3.26	0.00	3	1406.75058	0.46	29.45	0
	High	VSTVSPTTSVSGDR	1	1	1	TGME49_233220		0.0000	2.95	0.00	2	1392.69744	0.62	30.20	0
	High	FSAENEAVDKPR	1	1	1	TGME49_233220		0.0000	2.92	0.00	3	1362.66373	-0.85	29.93	0
	High	VSTVSPTTSVSGDRGER	2	1	1	TGME49_233220		0.0000	2.56	0.00	3	1734.86203	0.16	29.89	1
	High	TRENSLELPGVAIFDR	1	1	1	TGME49_233220		0.0000	2.56	0.00	3	1816.95554	0.14	34.99	1
	High	KQNSVLETPDVSQTR	1	1	1	TGME49_233220		0.0000	2.47	0.00	3	1701.87796	0.76	30.91	1
	High	TGmFGVGIPYSQHR	2	1	1	TGME49_233220	M3(Oxidation)	0.0000	2.37	0.00	3	1565.75479	1.16	32.54	0
	High	AAFAVDSSSADK	1	1	1	TGME49_233220		0.0000	2.32	0.00	2	1168.54680	-1.13	30.42	0
	High	VIESmVDPDSVcVHLLVK	1	1	1	TGME49_233220	M5(Oxidation); C12(Carbamidometh	0.0000	2.25	0.00	3	2056.05027	2.35	33.79	0
	High	LALVLTR	1	1	1	TGME49_233220		0.0000	2.19	0.00	2	785.52422	-0.22	32.85	0
	High	QNSVLETPDVSQTR	1	1	1	TGME49_233220		0.0000	2.14	0.00	2	1573.77995	-1.11	31.41	0

TGME49_311720	organism=Toxoplasma_gondii_ME49 | product=chaperonin protein BiP |	20.29	13.77	2	7	7	8	668	73.2	5.38

	A2	Sequence	# PSMs	# Proteins	# Protein Groups	Protein Group Accessions	Modifications	ΔCn	XCorr	Probability	Charge	MH+ [Da]	ΔM [ppm]	RT [min]	# Missed Cleavages
	High	IINEPTAAAIAYGLDKK	1	2	1	TGME49_311720		0.0000	3.04	0.00	3	1787.99100	0.41	33.64	1
	High	LADKIEEDDKK	1	1	1	TGME49_311720		0.0000	2.84	0.00	3	1303.67392	-0.11	29.15	2
	High	DKDLLPYEIINK	1	1	1	TGME49_311720		0.0000	2.78	0.00	3	1460.80066	0.74	33.87	1
	High	QVLEDADLQK	1	1	1	TGME49_311720		0.0000	2.63	0.00	2	1158.60039	0.21	30.91	0
	High	AKFEELNSDLFQK	1	1	1	TGME49_311720		0.0000	2.61	0.00	3	1568.79856	1.90	33.31	1
	High	NEATINPTNTLFDVK	2	1	1	TGME49_311720		0.0000	2.20	0.00	2	1676.85076	1.01	34.15	0
	High	ITPSYVAFTDDDRK	1	1	1	TGME49_311720		0.0000	2.12	0.00	3	1627.79422	-1.27	32.27	1

TGME49_219320	organism=Toxoplasma_gondii_ME49 | product=acid phosphatase GAP50	5.35	5.80	1	2	2	2	431	46.6	6.95

	A2	Sequence	# PSMs	# Proteins	# Protein Groups	Protein Group Accessions	Modifications	ΔCn	XCorr	Probability	Charge	MH+ [Da]	ΔM [ppm]	RT [min]	# Missed Cleavages
	High	LVSGTTGETLYTHK	1	1	1	TGME49_219320		0.0000	2.90	0.00	3	1506.78147	1.05	30.80	0
	High	ILDYIIVVADR	1	1	1	TGME49_219320		0.0000	2.44	0.00	2	1289.74785	1.11	35.17	0

TABLE S6

Accession	Description	Score	Coverage	# Proteins	# Unique Peptides	# Peptides	# PSMs	# AAs	MW [kDa]	calc. pI
TGME49_219320	organism=Toxoplasma_gondii_ME49 | product=acid phosphatase GAP50	98.93	34.57	1	13	13	28	431	46.6	6.95

A2	Sequence	# PSMs	# Proteins	# Protein Groups	Protein Group Accessions	Modifications	ΔCn	XCorr	Probability	Charge	MH+ [Da]	ΔM [ppm]	RT [min]	# Missed Cleavages
High	HSGSLYYAGETGFcLFELTAEGLVTR	2	1	1	TGME49_219320	C14(Carbamidomethyl)	0.0000	7.22	0.00	3	2878.37693	1.81	36.60	0
High	LAPADATEAAAAENHGYPK	4	1	1	TGME49_219320		0.0000	4.49	0.00	4	1896.90981	0.57	31.00	0
High	GDSmLQYYLQPLLK	2	1	1	TGME49_219320	M4(Oxidation)	0.0000	4.30	0.00	2	1684.86162	0.06	35.45	0
High	KSIDAFNFVSQLPEVR	2	1	1	TGME49_219320		0.0000	4.01	0.00	3	1849.98282	1.11	35.03	1
High	SIDAFNFVSQLPEVR	4	1	1	TGME49_219320		0.0000	3.98	0.00	2	1721.88408	-0.99	35.89	0
High	TELTYAVTSEQIKDGK	1	1	1	TGME49_219320		0.0000	3.80	0.00	3	1782.91330	0.70	31.61	1
High	LVSGTTGETLYTHKQPLK	2	1	1	TGME49_219320		0.0000	3.58	0.00	4	1973.07290	1.33	30.89	1
High	ILDYIIVVADR	2	1	1	TGME49_219320		0.0000	3.39	0.00	2	1289.74809	1.30	35.23	0
High	FVGLGNWGSGSYGQK	2	1	1	TGME49_219320		0.0000	3.20	0.00	2	1556.75127	1.28	33.82	0
High	LVSGTTGETLYTHK	3	1	1	TGME49_219320		0.0000	3.14	0.00	2	1506.77947	-0.28	30.58	0
High	TELTYAVTSEQIK	1	1	1	TGME49_219320		0.0000	2.90	0.00	2	1482.76995	0.87	32.74	0
High	TVADTLK	2	1	1	TGME49_219320		0.0000	2.71	0.00	1	747.42340	-1.78	29.46	0
High	TLELAPK	1	1	1	TGME49_219320		0.0000	2.01	0.00	1	771.46112	0.00	30.79	0

TGME49_266080	organism=Toxoplasma_gondii_ME49 | product=hypothetical protein | loc	17.19	9.62	1	6	6	6	728	81.1	8.72

A2	Sequence	# PSMs	# Proteins	# Protein Groups	Protein Group Accessions	Modifications	ΔCn	XCorr	Probability	Charge	MH+ [Da]	ΔM [ppm]	RT [min]	# Missed Cleavages
High	TALFAVEGVHASK	1	1	1	TGME49_266080		0.0000	3.38	0.00	3	1329.71674	0.41	32.39	0
High	VATEDIGVQTR	1	1	1	TGME49_266080		0.0000	3.09	0.00	2	1188.62248	0.45	30.46	0
High	SEQETESVSR	1	1	1	TGME49_266080		0.0000	2.76	0.00	2	1151.51811	0.51	28.55	0
High	NVFVAHVTQLR	1	1	1	TGME49_266080		0.0000	2.75	0.00	3	1283.72303	0.85	32.41	0
High	LIVLTHQDTIK	1	1	1	TGME49_266080		0.0000	2.62	0.00	3	1280.75782	0.39	31.79	0
High	LVQSQLNEQEVPLR	1	1	1	TGME49_266080		0.0000	2.59	0.00	2	1652.89629	-0.24	32.23	0

TGME49_235470	organism=Toxoplasma_gondii_ME49 | product=myosin A | location=TG	10.75	5.90	1	4	4	4	831	93.3	8.16

A2	Sequence	# PSMs	# Proteins	# Protein Groups	Protein Group Accessions	Modifications	ΔCn	XCorr	Probability	Charge	MH+ [Da]	ΔM [ppm]	RT [min]	# Missed Cleavages
High	LPSEEYQLGK	1	1	1	TGME49_235470		0.0000	2.82	0.00	2	1163.59441	0.07	31.14	0
High	NPVVAQLFAGIVmEK	1	1	1	TGME49_235470	M13(Oxidation)	0.0000	2.65	0.00	3	1631.88517	1.55	36.07	0
High	DGGIDDAAAIEGK	1	1	1	TGME49_235470		0.0000	2.64	0.00	2	1231.57610	-3.31	31.01	0
High	AEImEIVQQSK	1	1	1	TGME49_235470	M4(Oxidation)	0.0000	2.64	0.00	2	1291.65666	0.28	31.12	0

TGME49_223940	organism=Toxoplasma_gondii_ME49 | product=GAP45 | location=TGME4	18.56	20.00	1	4	4	6	245	27.3	5.07

A2	Sequence	# PSMs	# Proteins	# Protein Groups	Protein Group Accessions	Modifications	ΔCn	XCorr	Probability	Charge	MH+ [Da]	ΔM [ppm]	RT [min]	# Missed Cleavages
High	VAEHSSAAVTDR	1	1	1	TGME49_223940		0.0000	4.75	0.00	3	1242.60724	-0.10	28.61	0
High	cGcDLGDQHDENEcPIcR	1	1	1	TGME49_223940	C1(Carbamidomethyl); C3(Carbamid	0.0000	3.04	0.00	3	2234.82749	-1.97	30.44	0
High	NAADKAEAER	1	1	1	TGME49_223940		0.0000	2.77	0.00	3	1074.51725	-0.23	28.35	1
High	AEAAAAAER	3	1	1	TGME49_223940		0.0000	2.68	0.00	2	859.42693	0.05	27.99	0

TABLE S7

Accession	Description	Score	Coverage	# Proteins	# Unique Peptides	# Peptides	# PSMs	# AAs	MW [kDa]	calc. pI
TGME49_223940	organism=Toxoplasma_gondii_ME49 | product=GAP45 | location=TGME4	161.21	52.24	1	15	15	55	245	27.3	5.07

A2	Sequence	# PSMs	# Proteins	# Protein Groups	Protein Group Accessions	Modifications	ΔCn	XCorr	Probability	Charge	MH+ [Da]	ΔM [ppm]	RT [min]	# Missed Cleavages
High	LASPEDSASETTmATQPQK	1	1	1	TGME49_223940	M13(Oxidation)	0.0000	4.17	0.00	2	2007.92009	1.22	30.19	0
High	VAEHSSAAVTDR	6	1	1	TGME49_223940		0.0000	4.08	0.00	3	1242.60715	-0.17	28.54	0
High	RKAEAAAAAER	3	1	1	TGME49_223940		0.0000	3.82	0.00	3	1143.62281	-0.14	27.07	2
High	KAEAEAAEAER	3	1	1	TGME49_223940		0.0000	3.50	0.00	3	1174.57102	0.93	28.50	1
High	KEAEDLAEKER	1	1	1	TGME49_223940		0.0000	3.31	0.00	3	1317.66529	0.55	28.90	2
High	KAEAAAAAER	7	1	1	TGME49_223940		0.0000	3.28	0.00	2	987.52202	0.17	24.26	1
High	QmQEALKQEEmSPR	1	1	1	TGME49_223940	M2(Oxidation); M11(Oxidation)	0.0000	3.19	0.00	3	1736.79526	0.56	29.35	1
High	KEAEDLAEK	1	1	1	TGME49_223940		0.0000	3.14	0.00	2	1032.52178	0.91	28.64	1
High	AEAEAAEAER	1	1	1	TGME49_223940		0.0000	3.04	0.00	2	1046.47600	0.99	28.69	0
High	HIDLSDAPLLN	2	1	1	TGME49_223940		0.0000	3.02	0.00	2	1207.62871	-2.54	33.78	0
High	AAAEEAEQR	16	1	1	TGME49_223940		0.0000	2.98	0.00	2	974.45433	0.52	27.63	0
High	EAEDLAEKER	1	1	1	TGME49_223940		0.0000	2.75	0.00	3	1189.57056	0.81	29.08	1
High	SVVGYTVTPcDMASIDETAK	1	1	1	TGME49_223940	C10(Carbamidomethyl)	0.0000	2.73	0.00	3	2143.99198	1.53	32.59	0
High	VAEHsSAAVTDR	1	1	1	TGME49_223940	S5(Phospho)	0.0000	2.72	0.00	3	1322.57224	-1.10	28.83	0
High	AEAAAAAER	9	1	1	TGME49_223940		0.0000	2.69	0.00	2	859.42687	-0.02	27.16	0
High	NAADKAEAER	1	1	1	TGME49_223940		0.0000	2.63	0.00	2	1074.51848	0.92	28.29	1

TGME49_219320	organism=Toxoplasma_gondii_ME49 | product=acid phosphatase GAP50	42.14	31.09	1	10	10	13	431	46.6	6.95

A2	Sequence	# PSMs	# Proteins	# Protein Groups	Protein Group Accessions	Modifications	ΔCn	XCorr	Probability	Charge	MH+ [Da]	ΔM [ppm]	RT [min]	# Missed Cleavages
High	HSGSLYYAGETGFcLFELTAEGLVTR	1	1	1	TGME49_219320	C14(Carbamidomethyl)	0.0000	4.92	0.00	3	2878.37473	1.04	36.59	0
High	TELTYAVTSEQIKDGK	1	1	1	TGME49_219320		0.0000	3.79	0.00	3	1782.91239	0.19	31.56	1
High	LVSGTTGETLYTHK	1	1	1	TGME49_219320		0.0000	3.39	0.00	2	1506.77995	0.04	30.62	0
High	ILDYIIVVADR	1	1	1	TGME49_219320		0.0000	3.35	0.00	2	1289.74626	-0.12	35.19	0
High	LAPADATEAAAAENHGYPK	2	1	1	TGME49_219320		0.0000	3.33	0.00	4	1896.90639	-1.23	31.09	0
High	GDSmLQYYLQPLLK	2	1	1	TGME49_219320	M4(Oxidation)	0.0000	3.04	0.00	2	1694.86162	0.06	35.49	0
High	LVSGTTGETLYTHKQPLK	1	1	1	TGME49_219320		0.0000	2.99	0.00	4	1973.06875	-0.78	30.97	1
High	SIDAFNFVSQLPEVR	2	1	1	TGME49_219320		0.0000	2.91	0.00	2	1721.89275	4.04	35.78	0
High	FVGLGNWGSGSYGQK	1	1	1	TGME49_219320		0.0000	2.89	0.00	2	1556.75420	3.16	33.80	0
High	TELTYAVTSEQIK	1	1	1	TGME49_219320		0.0000	2.56	0.00	3	1482.76947	0.55	32.29	0

TGME49_235470	organism=Toxoplasma_gondii_ME49 | product=myosin A | location=TG	10.96	5.78	1	4	4	4	831	93.3	8.16

A2	Sequence	# PSMs	# Proteins	# Protein Groups	Protein Group Accessions	Modifications	ΔCn	XCorr	Probability	Charge	MH+ [Da]	ΔM [ppm]	RT [min]	# Missed Cleavages
High	ELIFTSNAEVIK	1	1	1	TGME49_235470		0.0000	2.95	0.00	2	1363.74565	-0.86	33.76	0
High	AEImEIVQQSK	1	1	1	TGME49_235470	M4(Oxidation)	0.0000	2.78	0.00	2	1291.65691	0.47	31.18	0
High	LPSEEYQLGK	1	1	1	TGME49_235470		0.0000	2.70	0.00	2	1163.59502	0.60	31.16	0
High	NPVVAQLFAGIVmEK	1	1	1	TGME49_235470	M13(Oxidation)	0.0000	2.53	0.00	3	1631.88553	1.77	36.05	0

TGME49_257680	organism=Toxoplasma_gondii_ME49 | product=myosin light chain MLC1	2.90	12.21	1	1	1	1	213	24.1	4.65

A2	Sequence	# PSMs	# Proteins	# Protein Groups	Protein Group Accessions	Modifications	ΔCn	XCorr	Probability	Charge	MH+ [Da]	ΔM [ppm]	RT [min]	# Missed Cleavages
High	FVGTSTHPEDNIEDLVEAFAYFDVSK	1	1	1	TGME49_257680		0.0000	2.90	0.00	3	2930.38053	2.51	36.63	0

TGME49_318230	organism=Toxoplasma_gondii_ME49 | product=phosphoglycerate kinase	2.60	3.12	1	1	1	1	417	44.6	6.99

A2	Sequence	# PSMs	# Proteins	# Protein Groups	Protein Group Accessions	Modifications	ΔCn	XCorr	Probability	Charge	MH+ [Da]	ΔM [ppm]	RT [min]	# Missed Cleavages
High	LGIQDVGAQLTGK	1	1	1	TGME49_318230		0.0000	2.60	0.00	2	1299.72795	0.92	33.52	0

TGME49_209030	organism=Toxoplasma_gondii_ME49 | product=actin ACT1 (ACT1) | loca	2.59	2.66	1	1	1	1	376	41.9	5.16

A2	Sequence	# PSMs	# Proteins	# Protein Groups	Protein Group Accessions	Modifications	ΔCn	XCorr	Probability	Charge	MH+ [Da]	ΔM [ppm]	RT [min]	# Missed Cleavages
High	AGVAGDDAPR	1	1	1	TGME49_209030		0.0000	2.59	0.00	2	928.44798	-0.39	28.92	0

TGME49_266080	organism=Toxoplasma_gondii_ME49 | product=hypothetical protein | loc	2.59	1.51	1	1	1	1	728	81.1	8.72

A2	Sequence	# PSMs	# Proteins	# Protein Groups	Protein Group Accessions	Modifications	ΔCn	XCorr	Probability	Charge	MH+ [Da]	ΔM [ppm]	RT [min]	# Missed Cleavages
High	VATEDIGVQTR	1	1	1	TGME49_266080		0.0000	2.59	0.00	2	1188.62261	0.55	30.42	0

TABLE S8

Accession	Description	Score	Coverage	# Proteins	# Unique Peptides	# Peptides	# PSMs	# AAs	MW [kDa]	calc. pI
TGME49_223940	organism=Toxoplasma_gondii_ME49 | product=GAP45 | location=TGME49_chrX:344	255.45	54.69	2	16	16	81	245	27.3	5.07

A2	Sequence	# PSMs	# Proteins	# Protein Groups	Protein Group Accessions	Modifications	ΔCn	XCorr	Probability	Charge	MH+ [Da]	ΔM [ppm]	RT [min]	# Missed Cleavages
High	cGcDLGDQHDENEcPIcR	2	1	1	TGME49_223940	C1(Carbamidomethyl); C3(Carbamid	0.0000	5.42	0.00	3	2234.83170	-0.09	30.34	0
High	RcGcDLGDQHDENEcPIcR	2	1	1	TGME49_223940	C2(Carbamidomethyl); C4(Carbamid	0.0000	4.77	0.00	3	2390.93442	0.59	30.17	1
High	LASPEDSASETTmATQPQK	3	1	1	TGME49_223940	M13(Oxidation)	0.0000	4.55	0.00	3	2007.91989	1.12	30.11	0
High	KAEAAAAAER	35	1	1	TGME49_223940		0.0000	3.93	0.00	2	987.52251	0.67	26.72	1
High	KEAEDLAEKER	1	1	1	TGME49_223940		0.0000	3.89	0.00	3	1317.66611	1.18	28.92	2
High	VAEHSSAAVTDR	8	1	1	TGME49_223940		0.0000	3.87	0.00	3	1242.60797	0.49	28.69	0
High	KEAEDLAEK	1	1	1	TGME49_223940		0.0000	3.83	0.00	2	1032.52190	1.02	28.63	1
High	RKAEAAAAAER	1	1	1	TGME49_223940		0.0000	3.53	0.00	3	1143.62326	0.26	27.66	2
High	HIDLSDAPLLN	3	1	1	TGME49_223940		0.0000	3.39	0.00	2	1207.63371	1.60	33.75	0
High	NAADKAEAER	2	1	1	TGME49_223940		0.0000	3.20	0.00	2	1074.51897	1.37	28.30	1
High	QmQEALKQEEMSPR	1	1	1	TGME49_223940	M2(Oxidation)	0.0000	3.10	0.00	3	1720.80173	1.37	30.03	1
High	KAEAEAAEAER	1	1	1	TGME49_223940		0.0000	3.07	0.00	3	1174.57019	0.22	28.49	1
High	QmQEALKQEEmSPR	1	1	1	TGME49_223940	M2(Oxidation); M11(Oxidation)	0.0000	2.92	0.00	3	1736.79636	1.19	29.39	1
High	AAAEEAEQR	11	1	1	TGME49_223940		0.0000	2.80	0.00	2	974.45458	0.77	27.86	0
High	AEAAAAAER	4	1	1	TGME49_223940		0.0000	2.78	0.00	2	859.42699	0.12	27.76	0
High	VAEHsSAAVTDR	1	1	1	TGME49_223940	S5(Phospho)	0.0000	2.66	0.00	3	1322.57425	0.42	28.84	0
High	EAEDLAEKER	1	1	1	TGME49_223940		0.0000	2.58	0.00	3	1189.57065	0.89	29.17	1
High	LAsPEDSASETTmATQPQK	1	1	1	TGME49_223940	S3(Phospho); M13(Oxidation)	0.0000	2.49	0.00	2	2087.88750	1.69	30.23	0
High	LASPEDSASETTMATQPQK	1	1	1	TGME49_223940		0.0000	2.44	0.00	2	1991.92571	1.50	30.64	0
High	AREEAER	1	2	1	TGME49_223940		0.1164	2.43	0.00	2	860.42119	-1.08	16.73	1

TGME49_219320	organism=Toxoplasma_gondii_ME49 | product=acid phosphatase GAP50 (GAP50) | l	20.30	12.99	1	4	4	7	431	46.6	6.95

A2	Sequence	# PSMs	# Proteins	# Protein Groups	Protein Group Accessions	Modifications	ΔCn	XCorr	Probability	Charge	MH+ [Da]	ΔM [ppm]	RT [min]	# Missed Cleavages
High	LVSGTTGETLYTHK	2	1	1	TGME49_219320		0.0000	3.34	0.00	3	1506.78119	0.86	30.61	0
High	TELTYAVTSEQIK	3	1	1	TGME49_219320		0.0000	3.17	0.00	2	1482.76933	0.45	32.51	0
High	FVGLGNWGSGSYGQK	1	1	1	TGME49_219320		0.0000	2.81	0.00	2	1556.74834	-0.61	33.71	0
High	GDSmLQYYLQPLLK	1	1	1	TGME49_219320	M4(Oxidation)	0.0000	2.76	0.00	2	1684.86174	0.13	35.44	0

TGME49_267430	organism=Toxoplasma_gondii_ME49 | product=DnaJ domain-containing protein | loc	19.23	14.35	1	5	5	6	425	48.9	8.82

A2	Sequence	# PSMs	# Proteins	# Protein Groups	Protein Group Accessions	Modifications	ΔCn	XCorr	Probability	Charge	MH+ [Da]	ΔM [ppm]	RT [min]	# Missed Cleavages
High	ASSQRPSQSETKPASATQK	2	1	1	TGME49_267430		0.0000	3.88	0.00	3	1989.00052	0.44	28.43	0
High	VAAAEASGGAVPQRPSGFSK	1	1	1	TGME49_267430		0.0000	3.72	0.00	3	1886.97287	0.46	30.54	0
High	KAQEVLmSDTR	1	1	1	TGME49_267430	M7(Oxidation)	0.0000	2.97	0.00	3	1293.64688	0.07	29.30	1
High	TmGTPSTAAIK	1	1	1	TGME49_267430	M2(Oxidation)	0.0000	2.75	0.00	2	1093.55754	1.55	29.70	0
High	AQEVLmSDTR	1	1	1	TGME49_267430	M6(Oxidation)	0.0000	2.72	0.00	2	1165.55266	0.72	29.64	0

TGME49_235470	organism=Toxoplasma_gondii_ME49 | product=myosin A | location=TGME49_chrX:4	16.35	4.09	1	4	4	5	831	93.3	8.16

A2	Sequence	# PSMs	# Proteins	# Protein Groups	Protein Group Accessions	Modifications	ΔCn	XCorr	Probability	Charge	MH+ [Da]	ΔM [ppm]	RT [min]	# Missed Cleavages
High	RALDNLHAVNK	1	1	1	TGME49_235470		0.0000	3.61	0.00	3	1250.69629	-0.13	29.95	1
High	ALDNLHAVNK	2	1	1	TGME49_235470		0.0000	3.45	0.00	3	1094.59586	0.48	30.14	0
High	ELIFTSNAEVIK	1	1	1	TGME49_235470		0.0000	3.09	0.00	2	1363.74614	-0.50	33.64	0
High	AEImEIVQQSK	1	1	1	TGME49_235470	M4(Oxidation)	0.0000	2.92	0.00	2	1291.65581	-0.38	31.27	0

TGME49_209030	organism=Toxoplasma_gondii_ME49 | product=actin ACT1 (ACT1) | location=TGME	10.13	11.97	2	4	4	4	376	41.9	5.16

A2	Sequence	# PSMs	# Proteins	# Protein Groups	Protein Group Accessions	Modifications	ΔCn	XCorr	Probability	Charge	MH+ [Da]	ΔM [ppm]	RT [min]	# Missed Cleavages
High	EEYDESGPSIVHR	1	1	1	TGME49_209030		0.0000	3.21	0.00	3	1517.68677	0.03	30.50	0
High	SYELPDGNIITVGNER	1	1	1	TGME49_209030		0.0000	2.80	0.00	2	1776.87724	0.51	33.57	0
High	AGVAGDDAPR	1	1	1	TGME49_209030		0.0000	2.44	0.00	2	928.44634	-2.17	28.88	0
High	GILTLK	1	2	1	TGME49_209030		0.0000	1.69	0.00	1	644.43451	0.52	32.18	0

TGME49_257180	organism=Toxoplasma_gondii_ME49 | product=RecF/RecN/SMC N terminal domain-	5.33	0.44	1	1	1	2	1588	181.2	6.65

A2	Sequence	# PSMs	# Proteins	# Protein Groups	Protein Group Accessions	Modifications	ΔCn	XCorr	Probability	Charge	MH+ [Da]	ΔM [ppm]	RT [min]	# Missed Cleavages
High	RAEEAER	2	1	1	TGME49_257180		0.0000	2.58	0.00	2	860.42095	-1.37	16.47	1

TGME49_300140	organism=Toxoplasma_gondii_ME49 | product=elongation factor 1-gamma, putative	3.10	4.31	1	1	1	1	394	44.0	6.30

A2	Sequence	# PSMs	# Proteins	# Protein Groups	Protein Group Accessions	Modifications	ΔCn	XCorr	Probability	Charge	MH+ [Da]	ΔM [ppm]	RT [min]	# Missed Cleavages
High	AAAKPAQSAGDDEEPAK	1	1	1	TGME49_300140		0.0000	3.10	0.00	3	1655.78519	-1.23	28.72	0

TGME49_257680	organism=Toxoplasma_gondii_ME49 | product=myosin light chain MLC1 | location=	3.04	12.21	1	1	1	1	213	24.1	4.65

A2	Sequence	# PSMs	# Proteins	# Protein Groups	Protein Group Accessions	Modifications	ΔCn	XCorr	Probability	Charge	MH+ [Da]	ΔM [ppm]	RT [min]	# Missed Cleavages
High	FVGTSTHPEDNIEDLVEAFAYFDVSK	1	1	1	TGME49_257680		0.0000	3.04	0.00	3	2930.37687	1.26	36.63	0

TGME49_268400	organism=Toxoplasma_gondii_ME49 | product=hypothetical protein | location=TGM	2.88	1.97	1	1	1	1	709	78.2	9.83

A2	Sequence	# PSMs	# Proteins	# Protein Groups	Protein Group Accessions	Modifications	ΔCn	XCorr	Probability	Charge	MH+ [Da]	ΔM [ppm]	RT [min]	# Missed Cleavages
High	RLEEVASKAEEKVR	1	1	1	TGME49_268400		0.0000	2.88	0.00	4	1643.89577	-7.20	28.59	3

TGME49_266080	organism=Toxoplasma_gondii_ME49 | product=hypothetical protein | location=TGM	2.51	1.51	1	1	1	1	728	81.1	8.72

A2	Sequence	# PSMs	# Proteins	# Protein Groups	Protein Group Accessions	Modifications	ΔCn	XCorr	Probability	Charge	MH+ [Da]	ΔM [ppm]	RT [min]	# Missed Cleavages
High	VATEDIGVQTR	1	1	1	TGME49_266080		0.0000	2.51	0.00	2	1188.62261	0.55	30.43	0

TABLE S9

Accession	Description	Score	Coverage	# Proteins	# Unique Peptides	# Peptides	# PSMs	# AAs	MW [kDa]	calc. pI
TGME49_267430	organism=Toxoplasma_gondii_ME49 | product=Dna2 domain-containing protein | location=TGME49_chrIX:656532-662192(+) | length=425 | sequence_SO=chron	47.73	25.41	1	11	11	20	425	48.9	8.82

A2	Sequence	# PSMs	# Proteins	# Protein Groups	Protein Group Accessions	Modifications	ΔCn	XCorr	Probability	Charge	MH+ [Da]	ΔM [ppm]	RT [min]	# Missed Cleavages
High	KAQEVLmSDTR	1	1	1	TGME49_267430	M7(Oxidation)	0.0000	3.22	0.00	2	1293.64714	0.27	29.45	1
High	TQQQQMTHLK	2	1	1	TGME49_267430		0.0000	2.98	0.00	3	1242.62629	0.25	29.44	0
High	NDILQAYR	3	1	1	TGME49_267430		0.0000	2.90	0.00	2	992.51702	1.02	32.08	0
High	AQEVLMSDTR	1	1	1	TGME49_267430		0.0000	2.67	0.00	2	1149.55681	-0.09	30.75	0
High	KAQEVLMSDTR	2	1	1	TGME49_267430		0.0000	2.49	0.00	2	1277.65557	2.88	30.42	1
High	VAAAEASGGAVPQRPSGPSK	1	1	1	TGME49_267430		0.0000	2.46	0.00	4	1886.97463	1.39	30.90	0
High	TmGTPSTAAIK	1	1	1	TGME49_267430	M2(Oxidation)	0.0000	2.46	0.00	2	1093.55657	0.66	29.83	0
High	ASSQRPSQSETKPASATQK	1	1	1	TGME49_267430		0.0000	2.41	0.00	4	1988.99941	-0.12	28.72	0
High	mTNEEFFMEIK	1	1	1	TGME49_267430	M1(Oxidation)	0.0000	2.27	0.00	2	1434.63030	1.57	34.47	0
High	TQQQQmTHLK	3	1	1	TGME49_267430	M6(Oxidation)	0.0000	2.26	0.00	3	1258.62091	0.02	28.37	0
High	AQEVLmSDTR	1	1	1	TGME49_267430	M6(Oxidation)	0.0000	2.23	0.00	2	1165.55278	0.82	29.76	0
High	mDEVLQR	1	1	1	TGME49_267430	M1(Oxidation)	0.0000	2.07	0.00	2	906.43486	-0.15	29.59	0
High	VTAYLK	1	1	1	TGME49_267430		0.0000	1.93	0.00	1	694.41376	0.48	30.19	0
High	FGDYK	1	1	1	TGME49_267430		0.0000	1.60	0.00	1	629.29327	0.48	29.47	0

Accession	Description	Score	Coverage	# Proteins	# Unique Peptides	# Peptides	# PSMs	# AAs	MW [kDa]	calc. pI
TGME49_235470	organism=Toxoplasma_gondii_ME49 | product=myosin A | location=TGME49_chrX:4884161-4889835(+) | length=831 | sequence_SO=chromosome | SO=protei	23.37	8.06	1	7	7	9	831	93.3	8.16

A2	Sequence	# PSMs	# Proteins	# Protein Groups	Protein Group Accessions	Modifications	ΔCn	XCorr	Probability	Charge	MH+ [Da]	ΔM [ppm]	RT [min]	# Missed Cleavages
High	RALDNLHAVNK	1	1	1	TGME49_235470		0.0000	3.24	0.00	3	1250.69703	0.46	30.28	1
High	YRDTFDLSK	2	1	1	TGME49_235470		0.0000	3.09	0.00	3	1144.56461	1.10	31.24	1
High	SQTIIVSGESGAGK	1	1	1	TGME49_235470		0.0000	2.97	0.00	2	1333.69670	0.64	30.60	0
High	ALDNLHAVNK	2	1	1	TGME49_235470		0.0000	2.63	0.00	3	1094.59549	0.15	30.32	0
High	GFQIWTDLAPSVK	1	1	1	TGME49_235470		0.0000	2.26	0.00	2	1461.77349	-0.15	35.66	0
High	LAPHVFYTAR	1	1	1	TGME49_235470		0.0000	2.24	0.00	3	1174.63620	-0.50	31.83	0
High	FHILPLSEYK	1	1	1	TGME49_235470		0.0000	2.22	0.00	3	1246.68280	-0.21	34.29	0

Accession	Description	Score	Coverage	# Proteins	# Unique Peptides	# Peptides	# PSMs	# AAs	MW [kDa]	calc. pI
TGME49_257680	organism=Toxoplasma_gondii_ME49 | product=myosin light chain MLC1 | location=TGME49_chrVIIb:3911290-3913592(+) | length=213 | sequence_SO=chromo	28.23	34.27	1	5	5	9	213	24.1	4.65

A2	Sequence	# PSMs	# Proteins	# Protein Groups	Protein Group Accessions	Modifications	ΔCn	XCorr	Probability	Charge	MH+ [Da]	ΔM [ppm]	RT [min]	# Missed Cleavages
High	FVGTSTHPEDNIEDLVEAFAYFDVSK	3	1	1	TGME49_257680		0.0000	5.66	0.00	3	2930.37870	1.88	36.80	0
High	LPNPADVLGPmDK	2	1	1	TGME49_257680	M11(Oxidation)	0.0000	3.20	0.00	2	1382.69890	0.28	33.62	0
High	QLGLAPSYADK	1	1	1	TGME49_257680		0.0000	2.25	0.00	2	1162.61431	3.44	31.62	0
High	SGDNLDYASFQK	1	1	1	TGME49_257680		0.0000	2.24	0.00	2	1344.60527	-1.05	31.83	0
High	VSTGDAm1LAR	1	1	1	TGME49_257680	M7(Oxidation)	0.0000	2.19	0.00	2	1149.59392	0.53	31.17	0
High	VSTGDAM1LAR	1	1	1	TGME49_257680		0.0000	2.14	0.00	2	1133.59990	1.33	32.36	0

Accession	Description	Score	Coverage	# Proteins	# Unique Peptides	# Peptides	# PSMs	# AAs	MW [kDa]	calc. pI
TGME49_223940	organism=Toxoplasma_gondii_ME49 | product=GAP45 | location=TGME49_chrX:3440541-3441278(-) | length=245 | sequence_SO=chromosome | SO=protein_co	6.59	9.39	1	2	2	2	245	27.3	5.07

A2	Sequence	# PSMs	# Proteins	# Protein Groups	Protein Group Accessions	Modifications	ΔCn	XCorr	Probability	Charge	MH+ [Da]	ΔM [ppm]	RT [min]	# Missed Cleavages
High	VAEHSSAAVTDR	1	1	1	TGME49_223940		0.0000	4.03	0.00	3	1242.60761	0.20	28.92	0
High	KAEAEAAEAER	1	1	1	TGME49_223940		0.0000	2.56	0.00	2	1174.56999	0.05	28.76	1

Accession	Description	Score	Coverage	# Proteins	# Unique Peptides	# Peptides	# PSMs	# AAs	MW [kDa]	calc. pI
TGME49_312990	organism=Toxoplasma_gondii_ME49 | product=DEAD/DEAH box ATP-dependent RNA helicase | location=TGME49_chrXI:3020716-3025702(-) | length=569 | seq	1.71	1.23	1	1	1	1	569	63.8	8.94

A2	Sequence	# PSMs	# Proteins	# Protein Groups	Protein Group Accessions	Modifications	ΔCn	XCorr	Probability	Charge	MH+ [Da]	ΔM [ppm]	RT [min]	# Missed Cleavages
High	DVLGAAK	1	1	1	TGME49_312990		0.0000	1.71	0.00	1	673.38788	-0.12	29.20	0

TABLE S10

Accession	Description	Score	Coverage	# Proteins	# Unique Peptides	# Peptides	# PSMs	# AAs	MW [kDa]	calc. pI
TGME49_257680	organism=Toxoplasma_gondii_ME49 | product=myosin light chain MLC1	124.70	81.22	1	10	10	43	213	24.1	4.65

A2	Sequence	# PSMs	# Proteins	# Protein Groups	Protein Group Accessions	Modifications	ΔCn	XCorr	Probability	Charge	MH+ [Da]	ΔM [ppm]	RT [min]	# Missed Cleavages
High	FVGTSTHPEDNIEDLVEAFAYFDVSK	3	1	1	TGME49_257680		0.0000	7.15	0.00	3	2930.38053	2.51	36.57	0
High	SGDNLDYASFQK	2	1	1	TGME49_257680		0.0000	3.70	0.00	2	1344.60820	1.13	31.84	0
High	ELNYFMWMPGFEWRPEPK	1	1	1	TGME49_257680		0.0000	3.51	0.00	3	2357.09269	1.86	36.53	0
High	VSTGDAMILAR	6	1	1	TGME49_257680		0.0000	3.33	0.00	2	1133.59978	1.22	32.34	0
High	KQmGNILmTYGEPLTTEEFNALAAEYF	1	1	1	TGME49_257680	M3(Oxidation); M8(Oxidation)	0.0000	3.27	0.00	3	4091.90659	4.29	36.46	1
High	VSTGDAmILAR	13	1	1	TGME49_257680	M7(Oxidation)	0.0000	3.18	0.00	2	1149.59477	1.28	31.12	0
High	LPNPADVLGPmDK	2	1	1	TGME49_257680	M11(Oxidation)	0.0000	3.05	0.00	2	1382.70012	1.16	33.32	0
High	EGGRPAADEDmQEALEEmVEADEMYA	1	1	1	TGME49_257680	M11(Oxidation); M18(Oxidation)	0.0000	2.64	0.00	3	3074.27085	1.52	33.54	0
High	QLGLAPSYADK	8	1	1	TGME49_257680		0.0000	2.60	0.00	2	1162.61150	1.02	31.59	0
High	HGYLTR	4	1	1	TGME49_257680		0.0000	2.23	0.00	2	746.39354	-1.17	29.41	0
High	LPNPADVLGPMDK	1	1	1	TGME49_257680		0.0000	2.15	0.00	2	1366.70085	-2.01	34.04	0
High	VGEYDGAcESPScR	1	1	1	TGME49_257680	C8(Carbamidomethyl); C13(Carbami	0.0000	2.05	0.00	2	1586.62053	-0.33	29.59	0

Supplementary Table 11: Oligonucleotides used in this study

S.No	Name of the primer	Oligo sequence
1	TgMLC1C8Arev	5'-tagcacaccggggctttcttctcgaccttgctcatct-3'
2	TgMLC1C11Afwd	5'-gaagaaatgcccggtggcctaccagaagctgccg-3'
3	TgMLC1C11Arev	5'-cggcagcttctggtaggccaccgggcatttcttc-3'
4	TgMLC1C8C11Afwd	5'-gagcaaggtcgagaagaaagccccggtggcctaccagaagctg-3'
5	TgMLC1C8C11Arev	5'-cagcttctggtaggccaccggggctttcttctcgaccttgctc-3'
6	TgMLC1C8Sfwd	5'-gagcaaggtcgagaagaaaagcccggtgtg-3'
7	TgMLC1C8Srev	5'-cacaccgggcttttcttctcgaccttgctc-3'
8	TgMLC1C11Sfwd	5'-aagaaatgcccggtgagctaccagaagctgc-3'
9	TgMLC1C11Srev	5'-gcagcttctggtagctcaccgggcatttctt-3'
10	TgMLC1C8SC11Sfwd	5'-gcaaggtcgagaagaaaagcccggtgagctaccaga-3'
11	TgMLC1C8SC11Srev	5'-tctggtagctcaccgggcttttcttctcgaccttgc-3'
12	PS235470-TyF	5'-aagttgaaacgaacgtgtctagaacgcg-3'
13	PS235470-TyR	5'-aaaacgcgttctagacacgttcgtttca-3'
14	MyoATy-Fwd	5'-gaaacgaacgtgtctagaacg-3'
15	MyoATy-Rev	5'-ggcggccagaaacaggtcggc-3'
16	MyoATy-Seq	5'-ctgacacatccccttcgtgcg-3'
17	pSS013-Fwd	5'-ccccgacacccgccaacacccg-3'
18	MyoAPS-Rev	5'-gcgttctagacacgttcgtttc-3'
19	MyoAgDNA-seqF	5'-cgtatatagtagcgatgtagg-3'
20	MyoATygDNA-F	5'-ctcgggaagacaatggttttc-3'
21	MyoATygDNA-R	5'-gagtggatcctggttcgtgtg-3'
22	MyoAgDNA-R	5'-gagccacggactgacaccatc-3'
23	HR MyoA-TyF2	5'-aatggatgagaagagttcaaaaggcaaacgaacgtgtctagagtggatcctggttcgtgtgaacttccaggaacgccggctgaacagtcgcggggctgacgttgttgtcc-3'
24	HR MyoA-TyR2	5'-ggacaacaacgtcagccccgcgactgttcagccggcgttcctggaagttcacacgaaccaggatccactctagacacgttcgtttgccttttgaactcttctcatccatt-3'
25	P1: TgMLC15'flankupstrFwd	5' -aatgtccgtagcaggcagca-3'
26	P2: GRA1BglIIRev	5'-gctagccgagatctcttgcttgatttcttcaaag-3'
27	P3: TgMLC1+1587(Exon3Start)Fwd	5'-cacaagtgaccagatcgactacag-3'
28	P4: TgMLC13'flankdownstr+829Rev	5'-cctttcaagtccgttcgcaacct-3'